Dissertation

ACYL-CHAIN DEPENDENT EFFECT OF LYSOPHOSPHATIDYLCHOLINE ON ENDOTHELIAL NITRIC OXIDE SYNTHASE AND NITRIC OXIDE BIOAVAILABILITY IN ENDOTHELIAL CELLS

submitted by

Andrijana KOZINA

mag.biol.mol.

for the Academic Degree of

Doctor of Philosophy

(PhD)

at the

Medical University of Graz

Institute of Molecular Biology and Biochemistry

under the Supervision of

Ao. Univ. Prof. Dr. Saša Frank

2014.

Declaration

I hereby declare that this thesis is my own original work and that I have fully acknowledged by name all of those individuals and organizations that have contributed to the research for this thesis. Due acknowledgements has been made in the text to all other material used. Throughout this thesis and in all related publications I followed the guidelines of “Good Scientific Practice”.

Graz, _____ _____

ACKNOWLEDGEMENTS

This dissertation reflects years of individual hard work, as well as the input of many generous and inspiring individuals that have helped me in various ways throughout this process. I would like to thank:

My supervisor, *Dr. Saša Frank*, for his continuous guidance and motivation throughout my studies that encouraged me to work with passion for science even in moments where nothing seemed to be going well.

The members of my thesis committee, *Dr. Dagmar Kratky* and *Dr. Gunther Marsche* for their time and useful comments.

Jay Patankar, for his guidance through the initial period of my PhD studies.

I would also like to thank my many colleagues at the Institute for Molecular Biology and Biochemistry for their help during this time, especially *Anton Ibovnik* for his technical support. Special thanks goes to the members of the Frank group: *Margarete Lechleitner*, *Michaela Gastrager, Shailaja Rao*, *Lada Brkić*, *Stefan Opresnik* and *Irene Schilcher* for all their help and scientific inputs, as well as their friendship, making it a really wonderful working environment.

I would like to acknowledge all collaborators from various institutes for their valuable contributions to this work.

Thanks to all my dear friends for their support, time, help and fun times, making this whole process so much more enjoyable.

And last, but not least, I would like to thank my family and fiancé for their love, encouragement and constant support every step of the way, for which I am truly grateful.

Table of Contents

ABBREVIATIONS

Ach- acetylcholine

ADMA - asymmetric dimethyl-L-arginine

ADP - adenine dinucleotide phosphate

BH_4 - tetrahydrobiopterin

BSA - bovine serum albumin

cGMP - cyclic guanosine monophosphate

CMC - critical micellar concentration

COX - cyclooxygenase

DAN - 2,3-diaminonaphthalene

DETCA – diethyldithiocarbamic acid diethylammonium salt

DHE - dihydroethidium

DMEM - Dulbecco's modified Eagle medium

EL - endothelial lipase

eNOS - endothelial nitric oxide synthase

FAD - flavin adenine dinucleotide

FBS - fetal bovine serum

FMN - flavin mononucleotide

H_2DCFDA - 2′,7′-dichlorodihydrofluorescein diacetate

HL - hepatic lipase

HPLC - high pressure liquid chromatography

IL-1ß - interleukin 1ß

HRP - Horseradish peroxidase

iNOS - inducible nitric oxide synthase

KPSS - physiological salt solution containing high amount of potassium

KO - knock out

LCAT - lecithin-cholesterol acyltransferase

LDL - low density lipoprotein

L-NA - nitro –L-Arginine

L-NNA - N_{ω}-Nitro-L-arginine

LPC - lysophosphatidylcholine

MTT - 3-(4,5-Dimethylthiazol-2-yl)-2,5-Diphenyltetrazolium Bromide

NADPH - nicotinamide dinucleotide phosphate

NAT - 2,3-naphthotriazole

nNOS - neuronal nitric oxide synthase

NO - nitric oxide

PBS - phosphate buffered saline

PC - phosphatidylcholine

PLA_2 - phospholipase A_2

PSS - physiological salt solution

PVDF - polyvinylidene flouride

RFP - red fluorescent protein

ROS - reactive oxygen species

sGC - soluble guanylyl cyclase

SOD- superoxide dismutase

TNFα -tumor necrosis factor alpha

WT- wild type

SUMMARY

Although it is known that LPC 16:0 modulates eNOS synthesis, NO production and promotes or impairs endothelium-dependent relaxation, little is known about unsaturated LPC species. Previous studies showed that the capacity of LPC 16:0, 18:1, 18:2 and 20:4 to induce endothelial prostacyclin production, interleukin-8 and cyclooxygenase-2 expression as well as potency of attenuating vasorelaxation were different depending on the acyl-chain length and degree of saturation.
The present doctoral thesis aimed to elucidate the possible acyl-chain dependent effects of LPC species, namely LPC 16:0, 18:1, 18:2 and 20:4 on endothelial nitric oxide synthase function and NO bioavailability in endothelial EA.hy 926 cell line.

The cells were acutely (15 minutes and 1 hour) exposed to 60 μM LPC species in a 5% FBS-containing medium, followed by examination of eNOS phosphorylation, dimer formation and activity, as well as quantification of nitrite levels, ROS formation and examination of NO bioavailability by functional bio-assays *ex vivo*.

Although LPC species caused no change in eNOS phosphorylation at both time points, the dimer to monomer ratio was decreased after exposure to LPC 16:0 and 18:1 at the 15-minute time point, and after exposure to LPC 16:0, 18:1 and 18:2 at the 1 hour time point. The change in dimer formation did not however affect the eNOS activity. The decrease in nitrite levels was observed at the 15-minute time point, but only LPC 18:1 caused a statistically significant decrease. Significant intracellular ROS formation was found after the 15- minute treatment of cells with LPC 16:0 and 18:1, but not with LPC 18:2 and 20:4. No elevation in ROS formation was observed at the 1-hour time point. The LPC 16:0-induced intracellular ROS was sensitive to NADPH oxidase inhibitor, and was localized predominately in the mitochondria. The LPC 16:0-induced ROS comprised of superoxide and other types of ROS, most probably hydrogen peroxide. The LPC 18:1-induced ROS was sensitive to NADPH oxidase, eNOS, xanthine oxidase and COX inhibitors, and localized in the mitochondria and cytoplasm. Intracellular and extracellular superoxide were predominant ROS triggered by LPC 18:1. The decrease in nitrite levels observed upon exposure of cells to LPC 18:1 could be ameliorated with the addition of Tiron, a superoxide scavenger.

The bio-assay *ex vivo* experiments showed that LPC 18:1 induced a marked decrease in NO bioavailability and impaired endothelium-dependent relaxation in mouse aortic rings. Those detrimental effects of LPC could be counteracted with Tiron.

The findings of this work denote LPC 18:1 as a potential inducer of endothelial dysfunction and suggest its role in subjects with high pathophysiological concentrations of LPC.

ZUSAMMENFASSUNG

LPC 16:0 ist als Modulator der eNOS Synthese, NO Produktion und als Hemmer und Förderer der Endothel-abhängigen Gefäßrelaxation bekannt. Im Gegensatz dazu ist wenig über die Funktion ungesättigter LPC-Spezies in diesem Zusammenhang bekannt. In Vorgängerstudien konnte gezeigt werden, dass die Fähigkeit der LPC Spezies 16:0, 18:1, 18:2 und 20:4 zur Induktion der Produktion von endothelialem Prostacyclin, Interleukin-8 und Cyclooxigenase 2 sich je nach Länger der Seitenkette und Sättigungsgrades unterschied.

Die vorliegende Dissertation beschäftigt sich mit Seitenketten-spezifischen Effekten der LPC Spezies 16:0, 18:1, 18:2, und 20:4 auf die Funktion von eNOS und die Bioverfügbarkeit von NO in der endothelialen EA.hy 926 Zelllinie.

Die Zellen wurden akut mit 60µm LPC Spezies in Medium mit 5% FBS behandelt, wonach eNOS Phosphorylierung, Dimer Bildung und Aktivität, und sowohl Nitrit Mengen und ROS Bildung als auch NO Bioverfügbarkeit mittels funktioneller *ex vivo* Bioassays gemessen wurden.

Obwohl sich die eNOS Phosphorylierung unter den verschiedenen LPC Spezies zu den untersuchten Zeitpunkten nicht unterschied, war die Dimer zu Monomer Ratio nach 15-minütiger Behandlung mit LPC 16:0 und 18:1 und nach 1-stündiger Behandlung mit LPC 16:0, 18:1 und 18:2 verringert. Diese Verringerung der Dimerisierung zeigte jedoch keinen Einfluss auf die eNOS Aktivität. Verringerte Nitrit Produktion zeigte sich nach 15 Minuten, jedoch resultierte nur die Behandlung mit LPC 18:1 in einem statistisch signifikanten Rückgang. Weiters zeigte sich eine signifikante intrazelluläre ROS Produktion nach einer 15-minütigen Behandlung mit LPC 16:0 und 18:1, jedoch nicht nach Behandlung mit 18:2 und 20:4. Die 1-stündige Behandlung führte zu keiner signifikanten ROS Produktion. Die durch LPC 16:0 hervorgerufene ROS Produktion war durch NADPH Inhibition zu unterbinden, fand sich vor allem im Bereich der Mitochondrien und setzte sich vor allem aus Superoxid und anderen ROS, mit größter Wahrscheinlichkeit Peroxid, zusammen. Im Gegensatz dazu, zeigte sich die durch LPC 18:1 induzierbare ROS Produktion durch NADPH, eNOS, Xanthin Oxidase und COX Inhibitoren hemmbar und trat vor allem im Bereich der

Mitochondrien und des Zytoplasmas auf. Intra- und extrazelluläres Superoxid waren die hier produzierten ROS. Der durch die Zugabe von LPC 18:1 hervorgerufene Rückgang in der Nitrit Produktion konnte durch den Superoxid Dismutase Hemmer Tiron verhindert werden.

Die ex vivo Bio-Assay Experimente mit murinen Aortenringen zeigten eine deutliche Abnahme der NO Bioverfügbarkeit sowie der Endothelium-abhängigen Vasodilatation hervorgerufen durch LPC 18:1. Diese nachteiligen Effekte von LPC 18:1 waren wiederum durch Tiron verhinderbar.

Die in dieser Arbeit aufgezeigten Erkenntnisse führen LPC 18:1 als eine mögliche Ursache vaskulärer Dysfunktion ins Treffen und zeigen seine mögliche Rolle in Personen mit pathologisch erhöhten LPC Spiegeln auf.

INTRODUCTION

Lysophosphatidylcholine

Lysophosphatidylcholine (LPC), 1-acyl-sn-glycero-3-phosphocholine, is a bioactive lipid derived from phosphatidylcholine (PC) by the selective loss of one fatty acyl residue (1). PC consists of a glycerol backbone, where the first two hydroxyl groups are esterified with two varying fatty acids (*sn*-1- and *sn*-2- position) and the third hydroxyl group is esterified with phosphatidylcholine (*sn*-3 position)(2). The majority of PCs occurring *in vivo* are characterized by a saturated fatty acyl residue on the *sn*-1 position, while the *sn*-2 position is often esterified with a moderately or highly unsaturated fatty acyl residue (3).

The LPC molecule is amphipathic in nature, consisting of one long hydrophobic fatty acyl chain and one large hydrophilic polar choline headgroup, which gives it surfactant and detergent-like properties; accordingly, LPC may lyse cells at high concentrations (4). LPCs are found in the circulation reversibly bound to albumin, lipoproteins or erythrocytes (5-7), with concentrations ranging from 120-190 μM under physiological conditions (8, 9), which can increase to milimolar concentration in hyperlipidemic subjects (10).

Both saturated and unsaturated LPC species are found in the human plasma, as phospholipases cleave the *sn*-1 or the *sn*-2 acyl residue. The circulating LPC is generated by a number of phospholipases. The phospholipase A_2 (PLA_2) family hydrolyzes PC on the *sn*-2 position generating LPC and arachidonic acid (11, 12). Lecithin-cholesterol acyltransferase (LCAT) also produces LPC by transferring a fatty acid from the *sn*-2 position of PC to cholesterol (13). While LCAT and PLA_2 generate saturated LPC species, *sn*-1 phospholipases such as endothelial lipase (EL) and hepatic lipase (HL) generate unsaturated LPC species (14, 15). The most abundant LPC in human plasma is palmitoyl-LPC (16:0-LPC), followed by linoleoyl- (18:2-LPC), oleoyl- (18:1-LPC) and arachidonoyl- LPC (20:4-LPC) (8, 16).

LPC is believed to play important roles in atherosclerosis and inflammatory diseases. LPC induces the production of adhesion molecules, chemoattractants and inflammatory mediators in endothelial cells (17-20), stimulates migration and proliferation of smooth muscle cells (21) and promotes endothelial dysfunction (22) thus causing disturbances in the vascular tone (23, 24).

Vascular endothelial cells

Vascular endothelial cells line the entire circulatory system and have very distinct and unique functions (25). As a barrier, the endothelium is semipermeable and regulates the transfer of small and large molecules. Endothelial cells exert significant endocrine, paracrine and autocrine actions and influence platelets, peripheral leukocytes and smooth muscle cells (26) (summary in Figure I-1).

The endothelium, under physiological conditions, prevents thrombosis by means of different anticoagulant and antiplatelet mechanisms (27). Endothelial cells also play a crucial role in regulating vascular tone, through production of several vasoactive mediators (28). Some compounds, such as endothelin, thromboxane A2, and angiotensin II are released to induce vascular contraction. Others, such as endothelium-derived nitric oxide (NO) and prostacyclin are released in response to hormones (catecholamines, vasopressin, aldosterone), physical stimuli, platelet-derived substances (serotonin, ADP), histamine, bradykinin and prostaglandins to induce vascular relaxation and inhibit platelet function (29, 30). Endothelial cells are also key players in host defense and inflammation; they produce and react to a number of cytokines and other mediators, modulating the activity of immune cells (26, 31).

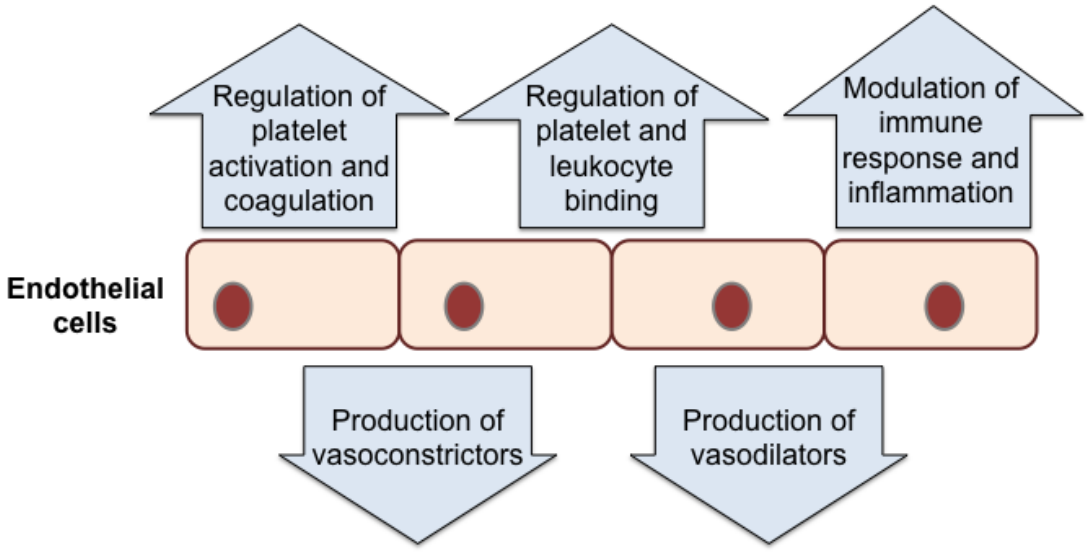

Figure I-1. Schematic summary of endothelial cell functions.

Endothelial nitric oxide synthase and NO

Molecular structure of eNOS

Endothelial nitric oxide synthase is an enzyme that generates NO from L-arginine. In mammal species, NO can be generated by three different isoforms of nitric oxide synthase: neuronal NOS (nNOS or NOS I), inducible NOS (iNOS or NOSII) and endothelial NOS (eNOS or NOS III) (32). eNOS is a 140 kDa large enzyme but the monomeric form is inactive. The formation of a dimer through the heme domains is required for activity. eNOS is predominantly located in the invaginations of the plasma membrane, the caveolae (33).

Several proteins interact with eNOS and regulate its activity. Caveolin-1, a caveolae coat protein, is an inhibitor of eNOS activity (34). Heat shock protein 90 (hsp 90) has been found to associate with eNOS and serves as an allosteric modulator activating the enzyme and promoting the coupling of eNOS. Ca^{2+} - activated calmodulin is important for the regulation of eNOS activity, and the activity of eNOS markedly increases with the increase of intracellular Ca^{2+}. The recruitment of calmodulin and hsp90 displaces caveolin-1, releasing eNOS from the caveolae, and leads to enzyme activation (35).

eNOS can also be regulated by phosphorylation on several serine (Ser), threonine (Thr) and tyrosine (Tyr) residues. Phosphorylation on Ser 1177, for example, increases the Ca^{2+} sensitivity of the enzyme and represents an additional mechanism of eNOS activation (36, 37). Phosphorylation on Thr495, however, is accompanied with the inhibition of eNOS activity, as it is phosphorylated under non-stimulated conditions and is likely to interfere with the binding of calmodulin to the enzyme (36).

eNOS has two major functional domains. The N-terminal catalytic domain binds the heme prosthetic group as well as tetrahydrobiopterin (BH_4), an important redox cofactor, and calmodulin. The C-terminal reductase domain has binding sites for flavin adenine dinucleotide (FAD), flavin mononucleotide (FMN) and nicotinamide dinucleotide phosphate (NADPH) (38). A functional eNOS transfers electrons from the reductase domain (from NADPH through FAD and FMN) to the heme in the N-terminal domain, where the electrons are used to reduce and activate oxygen and to oxidize L-arginine to L-citrulline (39).

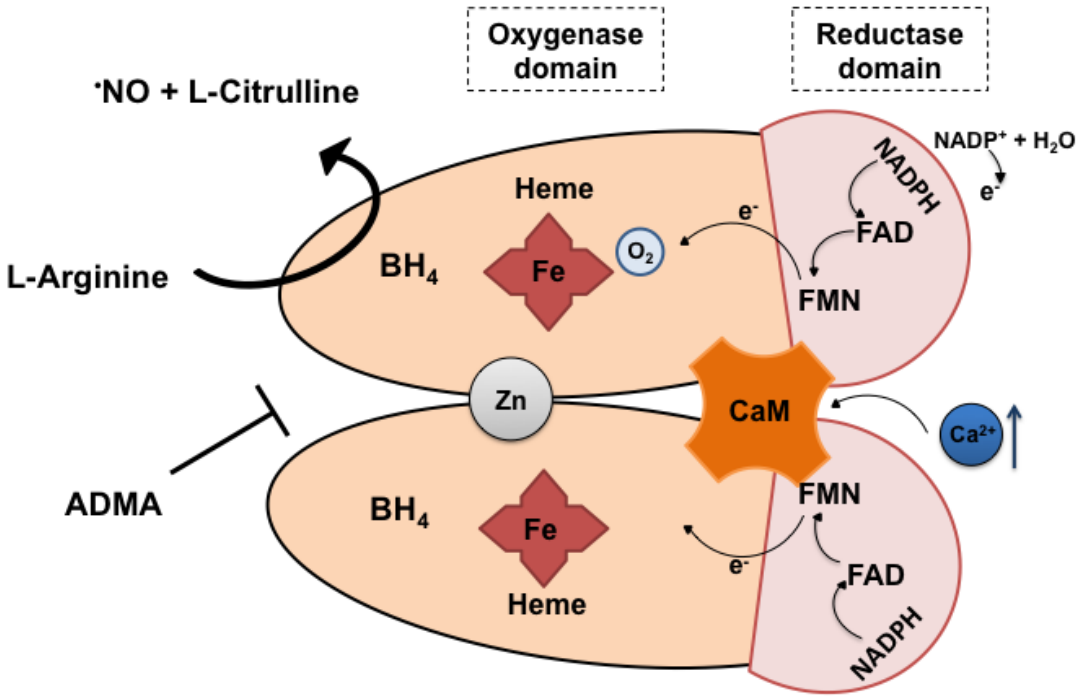

Figure I-2. Structure of the eNOS dimer. The electron travels from NADPH in the reductase domain via FAD and FMN to oxygen in the oxygenase domain that then oxidizes L-arginine to L-citrulline. Tetrahydrobiopterin (BH_4) is important as a redox cofactor, and it further stabilizes the dimer. Zink is responsible for connecting the monomers to the heme groups. Calmodulin (CaM) is a regulatory protein, where binding of Ca^{2+} to CaM activates eNOS, and the activity of the enzyme increases with the increase in intracellular calcium concentration. Asymmetric dimethyl-L-arginine inhibits eNOS activity, as it competes with L-arginine at the active site. Modified from (33).

Endogenous NOS inhibitors and eNOS uncoupling

Asymmetric dimethyl-L-arginine is an endogenous inhibitor of eNOS (40). ADMA belongs to a group of naturally occurring methylarginines, which are by-products of protein degradation in cells. ADMA competes with L-arginine at the active site and eNOS is no longer able to produce NO (41).

In states of increased oxidative stress, eNOS may become uncoupled. In this state, instead of producing NO, eNOS produces superoxide. Electrons normally flowing from the reductase domain of one subunit to the oxygenase domain of the

other subunit to L-Arg are diverted to molecular oxygen instead (42). There are several mechanism implicated in eNOS uncoupling. The most prominent is the oxidation of the critical NOS cofactor BH_4 by peroxynitrite ($ONOO^-$) that produces biologically inactive $BH3^\bullet$ radical (43, 44). Other suggested mechanisms are depletion of L-arginine and accumulation of endogenous methylarginines (32).

Nitric oxide

After being produced by NOS, NO has a half-life of only few seconds in an aqueous environment. NO is uncharged and highly soluble in hydrophobic environments, which allows it to diffuse freely across biological membranes (33). The end product of NO metabolism is nitrite, an inert and stabile compound, that can also serve as a substrate for NO production through nonenzymatic reduction, reaction with deoxyhemoglobin, or enzymatic reaction of oxidoreductases. However, under physiological conditions, nitrite does not function as an NO storage pool (45).

Nitric oxide largely functions through its interactions with heme moieties in a number of enzymes. One example is soluble guanylyl cyclase (sGC). Binding of NO to the heme in sGC activates the enzyme to produce cGMP, a second messenger responsible for the smooth muscle cell relaxation. NO can also bind to cysteins and thiols through nitrosation reactions, which are important post-translational changes that alter and regulate protein function (45).

NO has several vasculoprotective roles. Along with already mentioned vasodilation, NO inhibits platelet aggregation, prevents the release of platelet-derived growth factors that stimulate smooth muscle cell proliferation and production of matrix molecules, inhibits platelet, leukocyte and monocyte adhesion to the endothelium and is critical for adaptive vascular remodelling (32, 46).

In pathophysiologic states, NO reacts with reactive oxygen species (ROS) to form peroxynitrite and other reactive nitrogen species which can lead to nitration reactions that then mediate cell injury and death. Nitrotyrosine is one product of nitration reactions, and it is associated with numerous pathologic conditions.

Peroxynitrite is in general considered as a cytotoxic molecule; while in certain circumstances it can also provide vasodilatory effect (45, 47).

Reactive oxygen species

Reactive oxygen species are metabolites of oxygen that are produced as intermediates in reduction-oxidation reactions. Radicals derived from oxygen (and nitrogen) are the most important class of radical species generated in living systems (33). ROS include free radicals such as superoxide ($O2^{\bullet -}$), nitric oxide ($NO^{\bullet}$), and hydroxyl radical ($OH^{\bullet}$), and non-radicals such as hydrogen peroxide (H_2O_2) (48).

Superoxide

Superoxide is formed by the univalent reduction of molecular oxygen, has a half-life of only few seconds and is rapidly converted into H_2O_2 in a process that is accelerated by superoxide dismutase (SOD). Superoxide is generally restricted to the site of its production due to its poor cell membrane permeability. Superoxide can react with NO much faster than with SOD; accordingly, when both superoxide and NO levels are in the high nanomolar range, peroxynitrite is generated (48). Although superoxide production is linked to many pathological processes, there are also several conceivable physiological roles for endothelial superoxide such as oxygen sensing, regulation of vascular tone and effects on endothelial cell growth (49).

Hydrogen peroxide

Hydrogen peroxide is derived from the dismutation of superoxide or from the action of oxidases, such as glucose oxidase or xanthine oxidase. It is a small and non-polar molecule able to diffuse across biological membranes. H_2O_2 is a mild oxidant and relatively inert to most biomolecules, but it is able to induce reversible, covalent modifications of cysteine thiolate residues located in active sites of enzymes (50). Hydrogen peroxide is known to be involved in different aspects of endothelial cell function including endothelial cell growth and proliferation,

endothelial apoptosis, endothelial cytoskeletal reorganisation and barrier dysfunction and endothelium-dependent vasorelaxation. Therefore, pathophysiological changes in H_2O_2 concentration can lead to vascular disease (51).

Hydroxyl radical

Hydroxyl radical is a highly reactive radical. It is formed when hydrogen peroxide is reduced by one electron from a reduced metal such as iron or copper, in a process called Fenton reaction: $Fe^{2+} + H_2O_2 \rightarrow Fe^{3+} + {}^{\bullet}OH + OH^{-}$ (52). Hydroxyl radicals often initiate lipid peroxidation by abstracting a hydrogen atom from a fatty acid thus producing lipid peroxides (53).

Sources of ROS in the endothelial cell

There are several potential sources of ROS in the endothelial cell. The most important sources include NADPH oxidase, xanthine oxidase, mitochondria, cyclooxygenase and, above mentioned, uncoupled eNOS.

NADPH oxidase

The NADPH oxidase complex was originally identified and characterized in phagocytes, where it plays an essential role in non-specific host defense against microorganisms (54). The phagocytic enzyme is normally inactive, but becomes activated during the neutrophil oxidative burst to generate large amounts of superoxide (48).

The NADPH oxidase (Nox) family is composed of seven catalytic subunits termed Nox1-5 and Duox 1 and 2; regulatory subunits p22phox, p47phox, NoxO1, p67phox, NoxA1, p40phox and the major binding partner Rac (55).

Upon enzyme activation, regulatory subunits are translocated to and assemble with the membrane cytochrome. In the activated enzyme complex, the flavin-containing catalytic subunit functions as an electron transport system that uses NADPH as a donor of electrons that are ultimately transferred to molecular

oxygen, thus generating superoxide (56). Interestingly, superoxide is not the only ROS species being produced. In contrast to Nox1 and 2 that produce superoxide, Nox4 was shown to predominantly produce H_2O_2 (57).

Nox1, 2, 4 and 5 are expressed in cardiovascular tissues and participate not only in normal vascular function but also contribute to the development of cardiovascular diseases (55).

Nox2, also known as gp91phox, is the first discovered member of the NADPH oxidase. It is the catalytic subunit of the enzymatic complex responsible for the oxidative respiratory burst in phagocytes. Nox2 is also found throughout the cardiovascular system, where its activity and expression are much lower than in phagocytes (58). To form a fully functional NADPH oxidase, Nox2 requires additional proteins: p22phox, p67phox, p47phox, p40phox and Rac (57). In the resting state Nox2 is associated with p22phox forming a membrane complex know as cytochrome b558 (59). The other dormant subunits form a trimer in the cytosol with p67phox linking p47phox and p40phox (60). Extracellular stimuli induce a signaling cascade that activates Rac, p47phox and p40phox, causing translocation of cytosolic subunits to the membrane and association to the cytochrome to form an active enzyme (55). A schematic structure of Nox2 is depicted in Figure I-3. Because Nox2 releases superoxide, its cellular localization is important for its function. Nox2 is thought to be predominantly expressed at the plasma membrane (57), but it is also found in the intracellular compartments, around the nucleus (55). Nox2 seems to have a dual function in the vasculature. Under normal, physiological conditions it is involved in signal transduction of a large number of hormones, cytokines, and growth factors. However, under pathological conditions such as ischemia or diabetes, Nox2 becomes overly active generating large amounts of ROS that cause oxidative stress (57, 61).

Nox1 is expressed in a variety of cell types, including vascular smooth muscle cells and endothelial cells. There are two cytosolic subunits necessary for Nox1 activation. One is Nox Organizer 1 (NoxO1) that has the same role as p47phox, while the other is Nox Activator 1 (NoxA1), similar to p67phox (62). Similar to Nox2, Nox1 depends on the membrane subunit p22phox, as well as the activating

protein Rac1, which triggers the Nox-1 dependent ROS production (57). A schematic structure of Nox1 is depicted in Figure I-3. Nox1 can be found at the plasma membrane, in caveolae and in endosomes. Agonists appear to stimulate Nox1 in specific locations, thus determining where superoxide is produced: extracellularly by muscarinic agonists and thrombin, in endosomes by IL-1ß and TNFα; both inside and outside of cells by angiotensin II (62).

Nox4 is expressed almost ubiquitously, including the cardiovascular system and macrophages (63). Nox4 is usually co-expressed with other homologues like Nox1 and Nox2, but at significantly higher levels (55). Similarly to Nox1 and Nox2, Nox4 requires p22phox for its activity; however, the enzyme is independent of the cytosolic subunits. The binding site for Rac protein was not found in Nox4, indicating that it is a constitutively active enzyme (64). A schematic structure of Nox4 is depicted in Figure I-3. Nox4 can produce a higher hydrogen peroxide to superoxide ratio than Nox1 and Nox2, but it is yet to be determined whether it produces H_2O_2 directly or by superoxide dismutation. The subcellular distribution is wide, including endoplasmic reticulum, plasma membrane, nucleus and mitochondria (55).

Nox5 is found in vascular smooth muscle cells, endothelial cells and whole vessels. Unlike other mentioned Nox homologues, Nox5 does not require p22phox, cytosolic subunits or Rac (in some systems) for its activation. It has an additional cytosolic segment, a Ca^{2+}-binding domain (55). Although it is independent of the cytosolic subunits, it forms oligomers (tetramers) by self-association. It requires activation through calcium-induced conformational changes, direct phosphorylation and interaction with membrane phospholipids in order to produce superoxide (65). A schematic structure of Nox5 is depicted in Figure I-3.

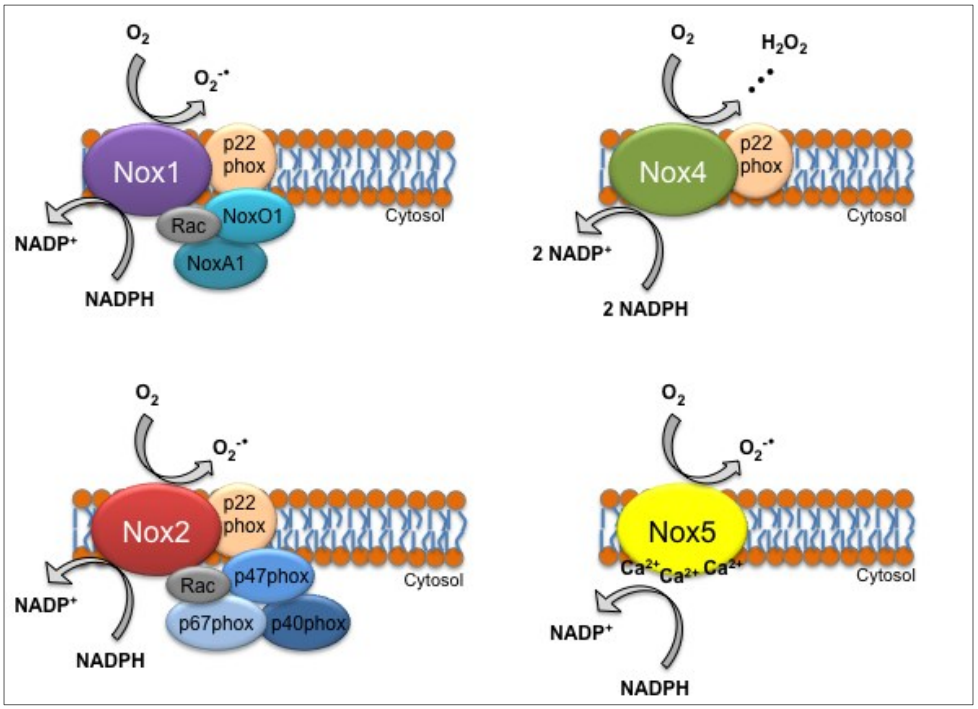

Figure I-3. Structure of NADPH oxidases found in endothelial cells. Nox1 requires p22phox, Rac, NoxO1 and NoxA1 protein for its activation; Nox2 requires p22phox, Rac, p47phox, p60phox and p40phox for its activation; Nox4 requires only p22phox, while Nox5 requires no additional proteins for its activation and is calcium dependent. Modified from (57))

Xanthine oxidase

Xanthine oxidase is an iron sulfur molybdenum flavoprotein with multiple functions. The enzyme exists in two forms, xanthine dehydrogenase and –oxidase, of which the former is predominant (53). Both xanthine dehydrogenase and –oxidase catalyze oxidation of hypoxanthine to xanthine and xanthine to urate. However, xanthine oxidase requires molecular oxygen as an electron acceptor, generating superoxide, whereas xanthine dehydrogenase requires NAD^+ (49). Xanthine dehydrogenase is converted to xanthine oxidase either through oxidation or by a proteolytic cleavage of a segment of xanthine dehydrogenase during hypoxia, ischemia or in the presence of proinflammatory mediators (48, 49).

Mitochondria

Mitochondria are organelles that provide energy to the cell through oxidative phosphorylation. In that process ATP is formed as electrons are transferred from NADH or $FADH_2$ to molecular oxygen. This occurs on the inner mitochondrial membrane through a series of electron transport carriers (66). Under pathological conditions, such as oxidative damage, mitochondrial oxidative phosphorylation can become uncoupled and result in the generation of superoxide (53). Increased oxidative damage within mitochondria may also contribute to greater lipid peroxidation and damage to cell membranes and DNA. In addition to the electron transport system, mitochondria also generate hydrogen peroxide through monoamine oxidase, an enzyme responsible for catecholamine metabolism, bound to the outer mitochondrial membrane (67).

Cyclooxygenase

Cyclooxygenase (COX) is an enzyme that catalyzes the first two steps in the biosynthesis of prostaglandins from arachidonic acid. There are two isoforms: the constitutive COX-1 and inducible COX-2 isoform (68). COX-1 has been implicated in ROS production in cells stimulated with TNF-α, interleukin-1 and bacterial lipopolysaccharide (69).

Oxidative stress and antioxidant enzyme systems

Oxidative stress is a consequence of an increase in the production and/or a decrease in the elimination of reactive species (33). Oxidative modifications within the arterial wall that may initiate or contribute to the development of endothelial dysfunction or atherosclerosis likely occur when the balance between oxidants and antioxidants shifts in favor of the former (53). Therefore it was important for the organisms to develop defense mechanisms via antioxidant agents. Defense mechanisms include enzymatic (SOD, catalase, glutathione peroxidases, thioredoxin) and non-enzymatic (ascorbic acid, tocopherol, glutathione, folic acid, etc.) antioxidants (33).

Superoxide dismutase

SODs are a major cellular defense system against superoxide in all vascular cells. The enzymes contain a redox metal in the catalytic center and dismutase superoxide radical to H_2O_2 and O_2 (53). There are three different isoforms of SOD that have been identified: the mitochondrial manganese-containing SOD (MnSOD), the cytosolic copper/zinc-containing SOD (CuZnSOD), and the extracellular SOD (ecSOD) (70).

Catalase

Catalase is an intracellular enzyme mainly located in cellular peroxisomes, and to some extent, in the cytosol. It catalyzes the two-step reaction of converting hydrogen peroxide to water and molecular oxygen. Catalase is very effective in high-level oxidative stress and protects cells from hydrogen peroxide produced within the cell (71).

Glutathione peroxidase

Glutathione peroxidase is a selenium-containing antioxidant enzyme that effectively reduces hydrogen peroxide and lipid peroxides to water and lipid alcohols, respectively, and in turn oxidizes glutathione to glutathione disulfide. The glutathione peroxidase/glutathione system is a major defense in low-level oxidative stress (53, 71).

Endothelial dysfunction

Endothelial dysfunction is characterized by a shift in the actions of the endothelium toward reduced vasodilation, a proinflammatory state, and prothrombic properties (25). Chronic dysfunction of the endothelium is implicated in the pathophysiology of several cardiovascular disorders including atherosclerosis, hypertension, diabetic vasculopathy and heart failure (49). When the ability of endothelial cells to release NO is reduced, and in particular if the propensity to produce endothelium-derived contracting factors is enhanced, endothelial dysfunction ensues, which appears to be the first step in the chain of events that leads to pathological states, thus endothelial dysfunction has become a hallmark and a predictor of cardiovascular disease (72).

Increases in oxidative stress in the cells are associated with reduced endothelium-dependent relaxation due to NO scavenging by ROS. Aging reduces endothelium-dependent vasorelaxation due to the reduced release and bioavailability of NO, and an increase in the release of vasoconstrictor prostaglandins. Active and passive smoking, chronic exposure to air pollution, as well as hypercholesterolemia and obesity also blunt endothelium-dependent vasodilatation (25, 30, 73, 74).

The normal endothelial turnover is accelerated by cardiovascular risk factors including hypertension and diabetes. The apoptotic cells are removed by the blood stream and replaced by regenerated endothelium formed by neighboring cells and/or circulating endothelial progenitor cells (75). However, the regenerated endothelium is dysfunctional (30). Experiments in porcine coronary arteries, where endothelium was damaged and allowed to regenerate, showed a marked blunting of the relaxations to aggregating platelets, serotonin and thrombin (all act via the pertussis–sensitive Gi-protein) (76, 77). On the contrary, relaxations evoked by bradykinin and ADP (which both depend on the Gq-signaling) and calcium ionophore A23187 were normal, showing the ability of the regenerated cells to produce NO. These observations implied a selective dysfunction of the Gi-dependent responses in regenerated endothelial cells (72). Primary cultures derived from regenerated endothelial cells had markers of accelerated senescence, a reduced expression and activity of eNOS, a greater production of ROS; the cells took up more low-density lipoproteins (LDL), and generated more

oxidized LDL (78, 79). In such a state, the NO deficiency permits the inflammatory reactions leading to atherosclerosis (30). The shortage of NO also unleashes the production of endothelium-derived prostanoids. These prostanoids activate receptors on the vascular smooth muscle cells leading to vasoconstriction, which amplifies the degree of endothelial dysfunction (72).

Aim

Although it is known that LPC 16:0 modulates eNOS synthesis (both increase and decrease have been described) (80, 81), NO production (82, 83) and is known to promote or impair endothelium-dependent relaxation (23), little is known about the impact of unsaturated LPC species on eNOS and NO bioavailability.

Previous studies showed that the capacity of LPC 16:0, 18:1, 18:2 and 20:4 to induce endothelial prostacyclin production (84), interleukin-8 (20) and cyclooxygenase-2 expression (19) as well as potency of attenuating vasorelaxation (24) were remarkably different depending on the acyl-chain length and degree of saturation.

The present doctoral thesis aimed to elucidate the possible acyl-chain dependent effects of LPC species, namely LPC 16:0, 18:1, 18:2 and 20:4 on eNOS function and NO bioavailability in endothelial EA.hy 926 cell line.

For that purpose, we designed experiments to mimic pathophysiological conditions where LPC concentrations are higher than in a healthy state. We acutely exposed cells (15 min, 1h) to LPC species and thereafter evaluated changes in:

- eNOS expression and activity
- NO bioavailability
- ROS production

To confirm our findings in cell culture, additional experiments were done *ex vivo* in mouse aortic rings.

MATERIAL AND METHODS

Material

Chemical	Company
Allopurinol	Sigma
apocynin	Sigma
$CaCl_2$	Roth
2′,7′-dichlorodihydrofluorescein diacetate (H_2DCFDA)	Biotium, Hayward, CA
Diethyldithiocarbamic acid diethylammonium salt (DETCA)	Sigma
Dihydroethidium (DHE)	Sigma
3-(4,5-Dimethylthiazol-2-yl)-2,5-Diphenyltetrazolium Bromide (MTT)	Sigma
DMSO	Merck
α-D-Glucose	Sigma-Aldrich
HCl	Roth
Indomethacin	Sigma
Isopropanol	Roth
KH_2PO_4	Merck
KCl	Roth
LPC 16:0, 18:1 and 18:2	Avanti Polar Lipids
LPC 20:4	Made by Martin Hermansson
β-mercaptoethanol	Sigma
Methanol	Roth
$MgSO_4$	Fluka
$NaHCO_3$	Merck
NaCl	Roth
N_ω-Nitro-L-arginine (L-NNA)	Sigma
peqGOLD Protein Marker IV and VII	Peqlab
Protease inhibitor Cocktail	Sigma
PVDF membrane	Roth
RIPA buffer	Thermo Fisher Scientific

Sodium orthovanadate	Calbiochem
Tiron	Sigma
Triton-X-100	Sigma
VAS-2870	Enzo Life Sciences
Antibodies	
eNOS	BD Transduction Laboratories
pS1177 eNOS	BD Transduction Laboratories
α-tubulin	Cell Signaling

LPC preparation

Arachidonoyl- linoleoyl-, oleoyl-, palmitoyl- lysophosphatidylcholine (LPC 20:4, 18:2, 18:1 and 16:0, respectively) in chloroform were aliquoted and evaporated under argon or nitrogen until dry and stored at -20 °C until use. LPC aliquotes were dissolved in PBS to a 3mM concentration and used fresh for every experiment.

Methods

Cell culture

Human endothelial cell line EA.hy926 was cultured in Dulbecco's modified Eagle medium (DMEM) containing 10% fetal bovine serum (FBS) and 1% HAT Media Supplement (all Gibco, Life Technologies). Cell culture medium was supplemented with penicillin G sodium sulfate (100 units/ml), streptomycin sulfate (100 mg/ml), and amphotericin B (2.5 mg/ml) (all Gibco, Life Technologies). Cells were cultured in humidified atmosphere of 5% CO_2/95% air at 37 °C and were sub-cultured using 0.025% trypsin/0.01% EDTA. Cells were seeded in plates 24h before exposure to LPC.

LPC treatment

Ea.hy 926 cells were plated in 12-well dishes 24h before treatment (120 000/well). Cells were washed once with warm PBS (Gibco) and treated with 60 μM LPC or PBS (vehicle) dissolved in DMEM medium containing 5% FBS for 15 minutes or 1 hour. Cells were also exposed to 10 μM LPC 18:1 in medium without FBS for 15 min. Medium was collected for nitrite/nitrate measurements, and cells were washed two times with cold PBS and lysed in RIPA buffer supplemented with Protease Inhibitor Cocktail (1 μl/million cells) and sodium orthovanadate, a phosphatase inhibitor (100 μM). Protein amount was determined using a BCA protein assay kit (Calbiochem and Pierce Thermo Scientific).

MTT cell viability assay

3-(4,5-Dimethylthiazol-2-yl)-2,5-Diphenyltetrazolium Bromide (MTT) is reduced by mitochondria of living cells to purple formazan, making it appropriate to use as a cell viability indicator. To test if LPC species affect cell viability, cells were incubated with LPC species and PBS control as described above for 15 minutes and 1 hour, after which they were washed once with PBS and incubated for 90 minutes in a FBS free medium containing 0,5 mg/ml MTT. Cells were then lysed in 0,04 M HCl in absolute isopropanol, and lysate absorbance was measured in

duplicate at wavelengths of 570 nm (measure wavelength) and 630 nm (reference wavelength).

Western blot

Equal amounts of cell lysate protein samples were denatured and subjected to gel electrophoresis using 10% SDS-polyacrylamide gels followed by transfer to PVDF membrane (150 mA, 70 min). Proteins were detected by antibodies specific for total eNOS (1:1000 dilution in 5% fat free milk), phosphorylated eNOS (pS1177; pT495) (1:1000 dilution in 5% BSA) and α-tubulin (1:1000 dilution in 5% BSA) overnight, followed by a washing step and appropriate HRP-conjugated secondary antibodies (Dako) (2h, room temperature). Antibody binding was visualized using a Immobilon Western Chemiluminescent HRP Substrate. Densitometry analyses were carried out using Image Lab software (Bio Rad).

For eNOS dimer Western blot, protein samples were mixed with a 6x SDS loading buffer without β-mercaptoethanol and were put onto 4-15% gel (BioRad) without denaturation. The electrophoresis was done cold (4°C), followed by transfer to PVDF membrane (220 mA, 4,5 h). The remaining protocol was done as described for total eNOS.

eNOS activity measurement

Intracellular conversion of L-[^{3}H]arginine into L-[^{3}H]citrulline was measured as previously described (85). Briefly, cells grown in 6-well plates were washed and incubated at 37 ˚C with 50 mM Tris buffer, pH 7.4, containing 100 mM NaCl, 5 mM KCl, 1 mM $MgCl_2$, 3 mM $CaCl_2$, 5% (vol/vol) fetal bovine serum, L-[2,3-^{3}H]arginine (~10^6 dpm) and 60μM LPC or PBS as vehicle control. Reactions were terminated after 15 min by washing the cells with chilled Tris buffer (50 mM, pH 7.4), containing 100 mM NaCl, 5 mM KCl, 1 mM $MgCl_2$ and 0.1 mM EGTA. Subsequent to lysis of the cells with 0.01 N HCl, an aliquot was removed for determination of incorporated radioactivity. To the remaining sample, 200 mM sodium acetate buffer (pH 13.0) containing 10 mM L-citrulline was added (final pH ~5.0), and L-[^{3}H]citrulline separated from L-[^{3}H]arginine by cation exchange chromatography(ref).

eNOS activity measurements were done in collaboration with Kurt Schmidt, Ph.D. at the Institute of Pharmaceutical Sciences, University of Graz.

ROS measurements

ROS production was measured using 2′,7′-dichlorodihydrofluorescein diacetate (H_2DCFDA) dye (Biotium, Hayward, CA, USA) that measures all intracellular ROS,and is not specific for certain type of ROS. Cells grown in 12-well dishes were washed with warm PBS and incubated 20 minutes with 10 μM H_2DCFDA in PBS (37°C) with or without inhibitors (allopurinol (30 μM) , apocynin (100 μM), DETCA (20 μM), Indomethacin(20 μM), L-NNA (100 μM), Tiron (100 μM), VAS-2870 (10 μM)). The dye was then aspirated and cells were incubated for 15 minutes and 1 hour with 60 μM LPC species or PBS (vehicle) in 5% FBS medium (37°C). After LPC incubation, medium was aspirated, cells were washed once with cold PBS and lysed with 300 μL 3% (v/v) Triton X-100 in PBS with shaking on ice for 45 minutes. 50 μL of cold absolute ethanol was then added to the lysate to increase the solubilization of the dye and cells were lysed for additional 15 minutes. The lysates were then collected and centrifuged (10 min,13000 rpm, 4°C). Fluorescence was measured in duplicate in white or black 96-well plates at excitation an emission wavelenghts of 485 and 540 nm, respectively. Fluorescence was normalized to protein content and fluorescence of vehicle-treated cells was set as 1.

To measure superoxide production, dihydroethidium (DHE) (Sigma) was used. Cells were plated in 96-well dishes at a density of 20000/well or, in case of microscopy, onto a glas coverslip in a 6-well dish at a density of 250 000/well. 24 hours after plating, cells were washed with warm PBS and incubated for 10 min (37°C) with 15 μM DHE in PBS with the addition of 20 μM DETCA, a SOD inhibitor. The dye was then aspirated, washed with warm PBS and cells were treated 15 minutes with 60 μM LPC 18:1, LPC 16:0 or PBS (vehicle) in PBS with 5% FBS (37°C). Fluorescence was then measured in a multilabel counter in 96 well plates at excitation an emission wavelenghts of 405 and 570 nm, respectively (86). For microscopy, cells loaded with DHE and treated with LPC or PBS were imaged on a digital wide field imaging system, the Till iMIC (Till Photonics

Graefelfing, Germany) using a 40x objective (alpha Plan Fluar 40x, Zeiss, Göttingen, Germany), as described recently (87). For illumination of DHE at 405 nm a monochromator, the Polychrome V (Till Photonics) was used. Emission light was collected at 560 nm. Images were recorded with a charged-coupled device (CCD) camera (AVT Stringray F145B, Allied Vision Technologies, Stadtroda, Germany). For data acquisition and the control of the digital fluorescence microscope the live acquisition software version 2.0.0.12 (Till Photonics) was used. The average intensity of randomly selected single individual cells was extracted using the offline analysis software version 2.0.0.12 from Till Photonics.

The microscopy experiments were done in collaboration with Roland Malli and Wolfgang F. Graier at the Institute of Molecular Biology and Biochemistry, Medical University of Graz.

Confocal mycroscopy

High resolution imaging of subcellular structures was performed in cells loaded with H_2DCFDA (20 min incubation) expressing either endoplasmic reticulum-targeted or mitochondria-targeted RFP after a 15 minute incubation with 60 µM LPC 18:1 or PBS. Images were acquired with an array confocal laser scanning microscope, built on an inverse, fully automatic microscope equipped with VoxCell Scan® (VisiTech) and a 100× objective (Plan-Fluor 100×/1.45 Oil, Zeiss). H_2DCFDA was illuminated at 488 nm (120 mW diode laser, Visitron Systems) and emission was collected at 535 nm (ET535/30m, Chroma Technology Corp.). RFP was excited with 561 nm laser light (50 mW, VSLaserModul, Visitron Systems) and fluorescence was recorded at 630 nm (630/75, Chroma Technology Corp.). Emitted light was acquired with a CCD camera (CoolSNAP-HQ, Photometrics). Background correction and image overlay were performed using the MetaMorph 7.7.0.0 software.

Confocal microscopy was done in collaboration with Roland Malli and Wolfgang F. Graier at the Institute of Molecular Biology and Biochemistry, Medical University of Graz.

Amplex Red assay

Cells were plated in 12-well dishes 24 before the experiment. Cells were washed once with warm PBS, after which 300 µL of pre-warmed assay buffer (HEPES-buffered Tyrodes's solution (without FBS) containing 50 µM Amplex Red (Invitrogen) and 2U/mL Horse Radish Peroxidase (Sigma)) containing 10 µM LPC 18:1 or vehicle (PBS) was added onto cells for 15 minutes. Experiment was also done in the presence of catalase 300 U/mL and superoxide dismutase 75 U/mL (both Sigma) in order to detect catalase-specific peroxides and superoxide radicals in the medium. The buffer was then transferred to a black 96 well plate and fluorescence was measured at excitation and emission wavelengths of 540 and 580 nm, respectively. Relative fluorescence units were normalized to protein concentration. Final values represent catalase sensitive H_2O_2 values (middle value of samples with added catalase is subtracted from other measured values).

For mouse aortic ring experiments, rings were isolated in ice cold PSS (see Wire myography paragraph), incubated in the buffer for 40 minutes at 37°C in a black 96 well plate, after which medium was replaced and PSS medium (without FBS) containing 50 µM Amplex Red, 2U/mL Horse Radish Peroxidase and 10 µM LPC 18:1, LPC 16:0 or vehicle (PBS) was added onto rings for 15 min. The buffer was then transferred to a new well and fluorescence was measured at excitation and emission wavelengths of 540 and 580 nm, respectively. Relative fluorescence units were normalized to dry weight of the aortic ring.

Superoxide determination in mouse aortic rings

Aorta was isolated and cut into rings. Weight of the aortae was recorded for normalization. Rings were incubated with or without 10µM LPC for 15 minutes followed by 30 minutes of DHE (10 µM) in 37°C. DHE products were extracted from the aortic rings by adding 300 µL acetonitrile. Extracts were concentrated by centrifuging in a Speed Vac machine. Pellets were dissolved in 110 µL of HPLC loading buffer (10% acetonitrile + 0.1% TFA in water) and loaded for HPLC measurement (88).

Measurements were done by Katrin Schröder, Ph.D and by Michael Sze Ka Wong, Ph.D at the Institute of Cardiovascular Physiology, Faculty of Medicine, Goethe-University Frankfurt.

Nitrite measurement in mouse aortic rings

Mouse aortic rings were isolated from the thoracic aorta in ice-cold PSS buffer (see Wire myography paragraph), and each ring was put into a separate well of a 96 well plate. The rings were then left to warm up for 1 hour in a 37°C incubator. In the last 30 minutes, L-NNA was added onto some rings at the final concentration of 100 µmol/L. After 1 hour, the medium was replaced with fresh warm PSS (without FBS) containing 10µM LPC 18:1 or PBS (vehicle) with or without 100 µM L-NNA. After a 15-minute incubation period, media was collected and stored at -20°C, and mouse aortic rings were collected and stored at -80°C. Rings were then lyophilized and dry weight was measured.

Nitrite measurements

As an indicator for NO production, nitrite was determined according to a previously described (89) fluorometric high-performance liquid chromatography (HPLC) method utilizing the reaction of nitrite with 2,3-diaminonaphthalene (DAN) (Sigma-Aldrich, Vienna, Austria). NO is converted primary to nitrite in cell culture media and physiological salt solution, and therefor can be used as an indicator of NO production (whereas in oxygenated blood it is further converted to nitrate). In brief: 100 µL of the cell culture medium or PSS, obtained after LPC cell treatment or mouse aortic ring treatment, respectively, were incubated at 24°C with 10 µL of 316 µmol/L DAN (in 0.62 mol/L HCl) for 10 min, followed by addition of 5 µL of 2.8 mol/L NaOH (Roth, Karlsruhe, Germany). This reaction mixture was directly used for the chromatographic separation (injection volume: 20 µL) of the formed 2,3-naphthotriazole. Nitrite standards (range: 0-2 µmol/L) were derivatized accordingly. NAT was isocratically separated on a 5-µm ODS hypersil column (150x4.6 mm) guarded by a 5-µm ODS hypersil column (10x4.6 mm; Uniguard holder) with a 30 mmol/L sodium phosphate buffer (pH=7.5) containing 50% acetonitril (flow rate: 0.8 mL/min). Acetonitrile instead of methanol in the mobile phase led to superior stability and elution of NAT prior to DAN. Fluorescence was monitored at an excitation wavelength of 375 nm and an emission wavelength of 415 nm. The HPLC apparatus consisted of an L-2200 autosampler, a L-2130 HTA pump and a L-2480 fluorescence detector (all: VWR Hitachi). Detector signals were recorded with a personal computer. The program EZchrom Elite (Scientific

Software Inc., San Ramon, CA USA) was used for data requisition and analysis. The detection limit for nitrite was 10 pmol/mL. In all experiments for nitrite measurements cells and rings were in parallel treated with 100 µM L-NNA (eNOS inhibitor) in order to determine eNOS contribution to nitrite production. Nitrite values shown in results are eNOS specific, since L-NNA nitrite values were subtracted from the total nitrite measured in the medium. Nitrite values were then normalized to protein.

Nitrite measurements were done in collaboration with Seth Hallström, Ph.D. at the Institute of Physiological Chemistry, Medical University of Graz.

Wire myography

Aortic rings approximately 2 mm in length were cut from descending thoracic aorta. The arterial rings were positioned in small wire myograph chambers (Danish MyoTechnology, Aarhus, Denmark), which contained physiological salt solution (PSS) (114 mM NaCl, 4.7 mM KCl, 0.8 mM KH_2PO_4, 1.2 mM $MgSO_4$, 2.5 mM $CaCl_2$, 25 mM $NaHCO_3$ and 11 mM α-D-glucose pH 7.4) aerated with 5% CO_2/95% O_2 at 37°C. The myograph chambers were connected to force transducers for isometric tension recording (PowerLab, ADInstruments). The rings were heated in PSS buffer to 37°C. An initial preload of 10 mN was applied, and the rings were allowed to stabilize for 30 min. PSS containing 60 mM KCl (KPSS) was used to determine maximum contractility of the tissue. When the developed tension attained its peak value, the rings were relaxed by rinsing with the buffer. Next, the rings were pre-contracted with increasing concentrations of norepinephrine (NE) (1 nM–0.3 mM) (Sigma-Aldrich) to produce 80% of the maximum contraction achieved by 60 mM KCl, followed by endothelium-dependent relaxation to cumulatively increasing concentrations of acetylcholine chloride (ACh) (1 nM– 0.3 mM) (Sigma-Aldrich). After washout and equilibration, the rings were preincubated with 10 µM LPC in the presence or absence of inhibitors for 15 minutes, followed by one-dose contraction with NE to achieve a 80% maximal KPSS contraction. The rings were then relaxed with increasing concentrations of ACh, as described above. Relaxation values were expressed as a percentage of the NE-induced contraction.

Organ bath

NO availability was estimated from the constrictor response to the eNOS inhibitor Nω-nitro-L-arginine (L-NA, 300 µM) in aortic rings preconstricted to 10% of the maximal KCl constriction, using phenylephrine in the presence of diclofenac (10 µM) as described (90). Briefly, rings were preincubated with or without LPC 18:1 for 15 min, after which rings were preconstricted with phenylephrine. After establishing a stable contraction, 300 µM of L-NA was added to the rings, and the increase in contraction was measured. The results are expressed as a ratio between L-NNA contraction and NE contraction. Experiments with Nox4 knock-out mice were done as described previously (90).

Organ bath experiments were done by Katrin Schröder, Ph.D and by Michael Sze Ka Wong, Ph.D at the Institute of Cardiovascular Physiology, Faculty of Medicine, Goethe-University Frankfurt.

Statistical analysis

Experiments were performed at least three times and the data are represented as the mean ± standard error mean. Differences between groups were assessed using unpaired t-test or Mann-Whitney U test for non-parametric data when comparing two groups, One-way ANOVA with subsequent Tukey's test adjusted for multiple testing for more than two groups, and Two-way ANOVA followed by a Bonferroni post-hoc test for myography experiments (all using Graph Pad Prism 5 .0). Statistically significant differences between groups are indicated by *P*-values of < 0.05 (*), < 0.01 (**), or < 0.001 (***).

RESULTS

LPC treatment does not affect EA.hy926 endothelial cell viability

60 μM LPC treatment of cells for 15 minutes and one hour did not affect cell viability, as found by MTT test (Figure 1).

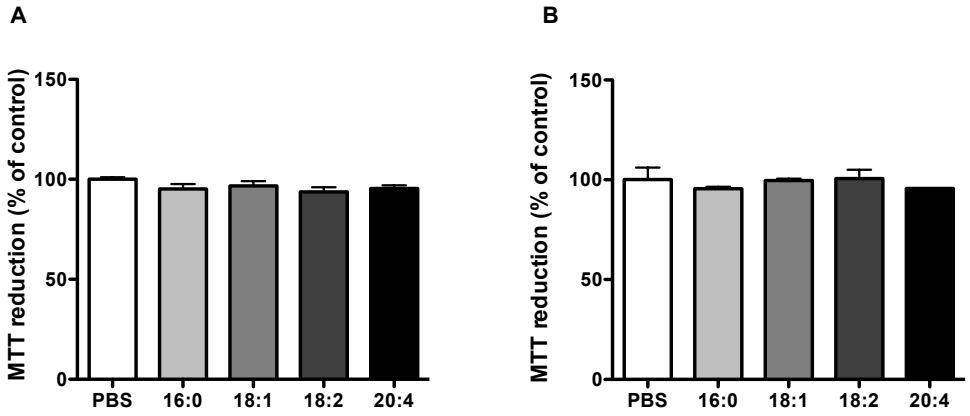

Figure 1. MTT cell viability test. Cells were exposed to 60 μM LPC 16:0, LPC 18:1, LPC 18:2, LPC 20:4 or vehicle (PBS) in a medium with 5% FBS for 15 minutes (A) and 1h (B), after which they were incubated with the MTT compound, and the intensity of the purple formazan product was measured spectrophotometrically. The MTT test showed that LPC species treatment had no negative effect on cell viability. Results are mean ± SEM of 3 independent experiments done in triplicates, and analyzed by one-way ANOVA with Tukey's post-hoc test.

LPC species have no effect on eNOS phosphorylation

eNOS phosphorylation serves as an indicator of eNOS activity, as phosphorylation on Ser1177 can further induce the activity of the enzyme. All LPC species, namely, LPC 16:0, LPC 18:1, LPC 18:2 and LPC 20:4, had no impact on eNOS phosphorylation on Ser1177 after 15 minute or 1 hour incubation, as shown in Figure 2.

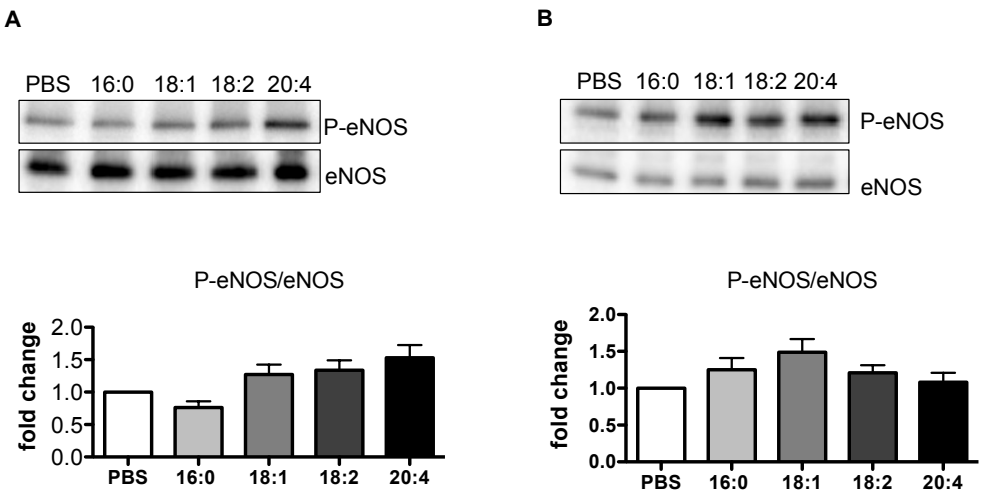

Figure 2. Western blots of total and phosphorylated eNOS from EA.hy926 cells treated with 60 µM LPC species. Cells were treated for 15 minutes or 1 hour with LPC species or vehicle control (PBS) in 5% FBS–containing medium. Equal amounts of protein were subjected to PAGE and transferred to a PVDF membrane and detected with appropriate antibodies. Treatment of EA.hy926 cells for 15 minutes (A) and 1 hour (B) had no significant effect on P-eNOS/eNOS ratio. Shown are representative blots and densitometric analysis of blots from at least 5 experiments done in duplicates. Results in graphs are mean values ± SEM and analyzed by one-way ANOVA with Tukey's post-hoc test.

LPC species affect nitrite levels in cell medium

In order to investigate the nitric oxide levels produced by cells, nitrite levels in the cell media were measured by HPLC. Nitrite is an indicator of NO production, as it is the end product of NO metabolism. After a 15 minute incubation with LPC species, LPC 16:0 and LPC 20:4 showed a tendency to decrease nitrite levels, however only the decrease of nitrite levels induced by LPC 18:1 was statistically significant (Figure 3.A). LPC 18:2 had no effect on nitrite levels. After 1 hour exposure to LPC species, LPC 16:0, LPC 18:1 and LPC 20:4 showed a tendency to reduce nitrite levels in cell media, however without reaching statistical significance (Figure 3.B)

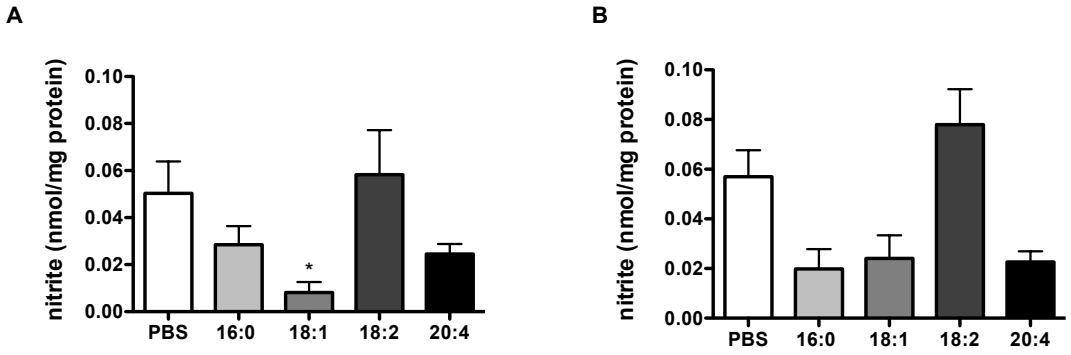

Figure 3. Nitrite levels in cell culture media from LPC - treated cells. Cells were treated with 60 µM LPC species and vehicle control (PBS) with or without 100 µM eNOS inhibitor L-NNA in 5% FBS-containing medium for 15 minutes (A) or 1 hour (B), after which medium was collected, and protein lysates were used for normalization. Nitrite was measured by HPLC. Although nitrite levels showed a tendency to be decreased after a 15 minute treatment (A) of EA.hy926 cells with LPC 16:0 and LPC 20:4, only the decrease in nitrite levels after exposure to LPC 18:1 was statistically significant compared to vehicle control. After 1 hour of treatment (B), there was no statistically significant lowering of nitrite levels compared to control. All nitrite values shown are eNOS specific, as nitrite values of cells treated with L-NNA (eNOS unspecific nitrite) were subtracted from all measurements. Results shown are mean values ± SEM of 3 independent experiments done in sextuplicates, and analyzed by one-way ANOVA with Tukey's post-hoc test. If otherwise not indicated, asterisks show significance compared to PBS control (*p<0,05).

LPC species exhibit an acyl-chain dependent effect on eNOS dimer

After 15 minutes of incubation with LPC species, LPC 16:0 and LPC 18:1 induced a decrease in the eNOS dimer/monomer ratio compared to PBS control, indicating LPC-induced uncoupling of eNOS (Figure 4.A). After 1 hour exposure to LPC species, LPC 18:2, along with LPC 16:0 and LPC 18:1 induced a decrease in the eNOS dimer/monomer ratio compared to control (Figure 4.B). LPC 20:4 showed no effect on eNOS dimer.

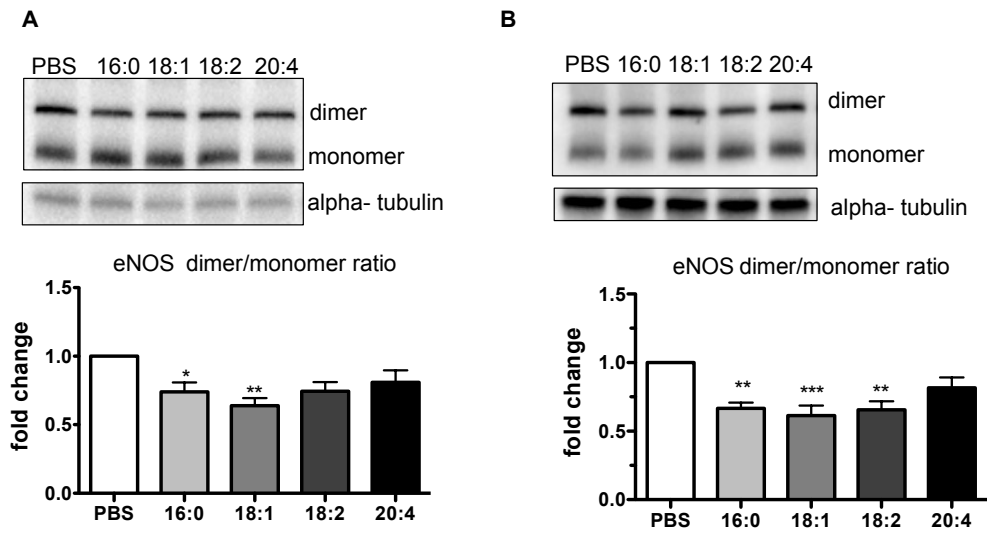

Figure 4. Western blots of eNOS dimer and monomer from EA.hy926 cells treated with 60 µM LPC species. Cells were treated for 15 minutes or 1 hour with LPC species or vehicle control (PBS) in 5% FBS-containing medium. Equal amounts of protein were mixed with sample buffer without β-mercaptoethanol, and PAGE was done cold (4°C), after which proteins were transferred to a PVDF membrane and detected with an appropriate antibody. The 15 minute treatment (A) with LPC 16:0 and LPC 18:1 had significantly decreased the eNOS dimer/monomer ratio, while after 1 hour of treatment (B) LPC 18:2, along with LPC 16:0 and LPC 18:1 had significantly decreased the eNOS dimer/monomer ratio. Here shown are representative blots and densitometric analysis of blots from at least 5 experiments done in duplicates. Results in graphs are mean values ± SEM and analyzed by one-way ANOVA with Tukey's post-hoc test. If otherwise not indicated, asterisks show significance compared to PBS control (*p<0,05, **p<0,01, ***p<0,001).

LPC species do not alter eNOS activity

To investigate whether the decrease of nitrite in the media is due to less NO production, eNOS activity was measured at the 15-minute time point. As shown in Figure 5, there was no significant decrease in eNOS activity after exposure of cells to LPC.

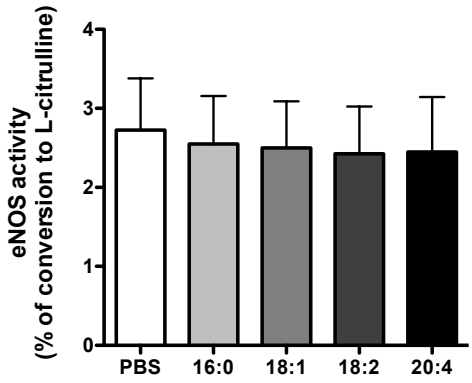

Figure 5. eNOS activity. Activity of the eNOS enzyme was determined in EA.hy926 cells exposed to 60 µM LPC species or vehicle control (PBS) along with L-[^{3}H]arginine in the presence of 5% FBS for 15 min followed by quantification of L-[^{3}H]citrulline after its separation from L-[^{3}H]arginine by exchange chromatography. There was no difference in eNOS activity after treatment with LPC species compared to control. Results shown are mean ± SEM, of 3 independent experiments performed in triplicates and analyzed by one-way ANOVA with Tukey's post-hoc test.

LPC induces intracellular ROS production

To test whether observed decreased nitrite levels were reflect ROS (superoxide)-mediated NO scavenging, intracellular ROS was measured using H_2DCFDA dye, that is susceptible to oxidation by a large number of different ROS species. As shown in Figure 6.A, LPC 16:0 and LPC 18:1 significantly increased intracellular ROS levels after a 15 minute incubation period. After 1 hour incubation with LPC species (Figure 6.B), no increase in intracellular ROS was found, but a decrease after exposure to LPC 18:2 and LPC 20:4. DETCA, a superoxide dismutase inhibitor, was used as a specificity control of the H_2DCFDA dye for superoxide. As the ROS levels with DETCA were decreased after 1h compared to control, it indicated the low sensitivity of the fluorescent H_2DCFDA dye for superoxide detection.

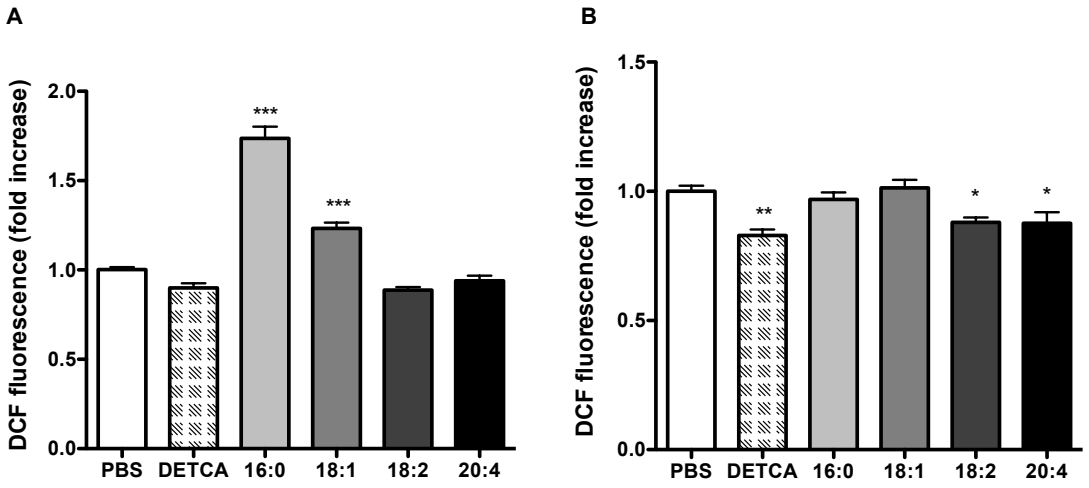

Figure 6. Intracellular ROS measurement in LPC-treated cells. EA.hy926 cells were preincubated with 10μM H_2DCFDA fluorescent dye with or without 20μM DETCA (SOD inhibitor), after which they were treated with 60μM LPC species or vehicle control (PBS) in 5% FBS medium for 15 minutes or 1 hour. Thereafter, cells were lysed and fluorescence was measured. After a 15 minute treatment (A), LPC 16:0 and LPC 18:1 significantly induced intracellular ROS levels. One hour treatment of cells with LPC species (B) did not increase intracellular ROS levels, however cells treated with LPC 18:2 and LPC 20:4 had a small but significant decrease in the intracellular ROS levels. Results shown are mean ± SEM, of 3 independent experiments performed in triplicates and analyzed by one-way ANOVA with Tukey's post-hoc test. If otherwise not indicated, asterisks show significance compared to PBS control (*p<0,05, **p<0,01, ***p<0,001).

As there was no induction of ROS and no significant decrease in nitrite levels at the 1 hour time point, we focused on the 15 minute time point to elucidate the type and source of ROS induced with LPC species. As LPC species 18:2 and 20:4 had no impact on either nitrite levels or ROS levels, we focused only on LPC species 16:0 and 18:1.

NADPH oxidase is involved in ROS formation

As NADPH oxidases are a major source of ROS, Nox4 and Nox1/2 inhibitors VAS-2870 and apocynin were used, respectively, to determine the involvement of these two NADPH oxidases in LPC-induced ROS. VAS-2870 was able to abolish both LPC 16:0- and LPC 18:1-induced ROS (Figure 7.A). In contrast, apocynin (Figure 7.B) had no impact on LPC - induced ROS production.

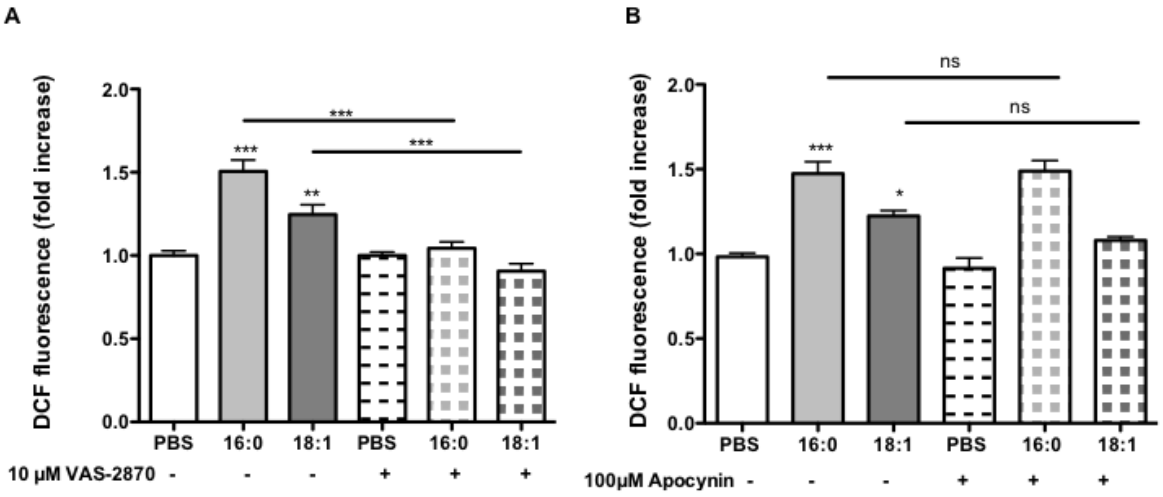

Figure 7. Involvement of Nox4 and Nox1/2 in LPC 16:0- and LPC 18:1-induced intracellular ROS production. EA.hy926 cells were preincubated with 10µM H_2DCFDA fluorescent dye with or without VAS-2870 (Nox4 inhibitor) and apocynin (Nox1/2 inhibitor), after which they were treated with 60µM LPC 16:0 and LPC 18:1 or vehicle control (PBS) in 5% FBS-containing medium for 15 minutes. Thereafter, cells were lysed and fluorescence was measured. Inhibition of Nox4 (A) abolished completely the intracellular ROS formation after treatment with LPC 16:0 and LPC 18:1. Inhibition of Nox1/2 (B) had no significant effect on ROS production induced by LPC 16:0 and LPC 18:1. Results shown are mean ± SEM, of 3 independent experiments performed in triplicates and analyzed by one-way ANOVA with Tukey's post-hoc test. If otherwise not indicated, asterisks show significance compared to PBS control (*p<0,05, **p<0,01, ***p<0,001, ns - not significant).

Involvement of eNOS, XO and COX in ROS production

eNOS inhibitor L-NNA, abolished LPC 18:1-, but only slightly attenuated LPC 16:0-induced ROS formation (Figure 8.A). Xanthine oxidase inhibitor allopurinol (Figure 8.B) failed to decrease LPC–induced ROS, but decreased the basal levels of ROS. This was obvious as a significant decrease in ROS in PBS - treated cells upon allopurinol treatment, compared with PBS-treated cells in the absence of allopurinol. Indomethacin, a cyclooxygenase inhibitor, was able to decrease LPC 18:1-induced ROS (Figure 8.C). LPC 16:0-induced ROS was significantly decreased after inhibition of COX, but it was still significantly higher than PBS control cells treated with indomethacin.

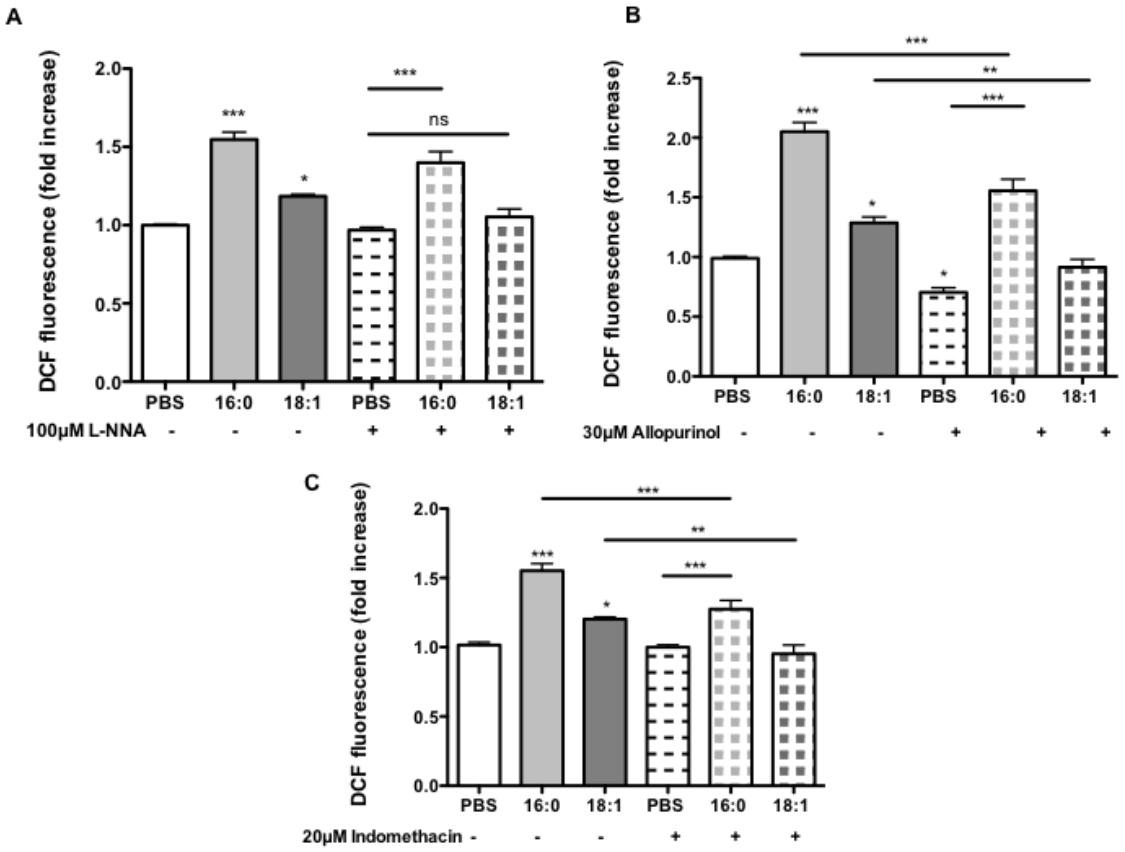

Figure 8. Involvement of eNOS, xanthine oxidase and cyclooxygenase enzymes in LPC 16:0- and LPC 18:1-induced intracellular ROS. EA.hy926 cells were preincubated with 10μM H_2DCFDA fluorescent dye with or without L-NNA (eNOS inhibitor), allopurinol (xanthine oxidase inhibitor) and indomethacin (COX inhibitor), after which they were treated with 60μM LPC 16:0 and LPC 18:1 or vehicle control (PBS) in 5% FBS-containing medium for 15 minutes. Thereafter,

cells were lysed and fluorescence was measured. Inhibition of eNOS (A) failed to attenuate LPC 16:0-induced ROS; however it suppressed the LPC 18:1-induced ROS. Inhibition of xanthine oxidase (B) lowered the basal levels of intracellular ROS, but not LPC -induced ROS formation. Inhibition of COX (C) partially lowered the LPC 16:0-induced ROS, but ROS levels were still higher than in control cells. LPC 18:1 -induced ROS was completely abolished by the inhibition of COX. Results shown are mean ± SEM, of 3 independent experiments performed in triplicates and analyzed by one-way ANOVA with Tukey's post-hoc test. If otherwise not indicated, asterisks show significance compared to PBS control (*p<0,05, **p<0,01, ***p<0,001, ns - not significant).

LPC 18:1- and LPC 16:0- induce production of different ROS species

To examine the nature of ROS species induced by LPC 16:0 and 18:1, the ROS levels were measured with H_2DCFDA (a dye that detects all intracellular ROS, primarily peroxide and peroxynitrite, and marginally superoxide), in the presence or absence of Tiron (a superoxide scavenger) or DETCA (a SOD inhibitor). As shown in Figure 9.A, Tiron abolished LPC 18:1-induced ROS, but only partially decreased (not significantly) the LPC 16:0-induced ROS. DETCA abolished LPC 18:1-induced ROS, and significantly decreased the LPC 16:0-induced ROS (Figure 9.B). Failure of both Tiron and DETCA to abolish LPC 16:0-induced ROS, in contrast to the abolished LPC 18:1-induced ROS with those inhibitors, indicates that: i0 LOC 18:1 induces exclusively superoxide which is converted by SOD to hydrogen peroxide and that ii) LPC 16:0 induces superoxide as well, but also a direct, SOD-independent production of ROS species detectable with H2DCFDA, most likely hydrogen peroxide.

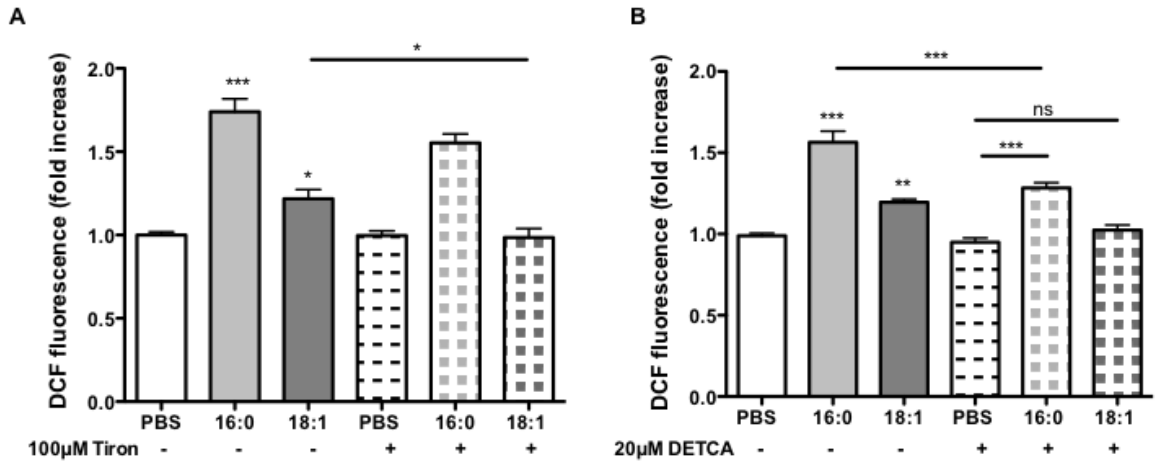

Figure 9. Effect of Tiron and DETCA on LPC 16:0- and LPC 18:1-induced ROS. EA.hy926 cells were preincubated with 10μM H_2DCFDA fluorescent dye with or without Tiron (superoxide scavenger), and DETCA (SOD inhibitor), after which they were treated with 60μM LPC 16:0 and LPC 18:1 or vehicle control (PBS) in 5% FBS-containing medium for 15 minutes. Thereafter, cells were lysed and fluorescence was measured. Superoxide scavenger Tiron abolished the LPC 18:1-induced ROS, however LPC 16:0-induced ROS was not affected (A). SOD inhibitor DETCA completely inhibited the LPC 18:1-induced ROS, and LPC 16:0-induced ROS was partially inhibited, but still higher compared to control (B). Results shown are mean ± SEM, of 3 independent experiments performed in triplicates and analyzed by one-way ANOVA with Tukey's post-hoc test. If otherwise not indicated, asterisks show significance compared to PBS control (*p<0,05, **p<0,01, ***p<0,001, ns - not significant).

Both LPC 16:0 and 18:1 induce superoxide production

To demonstrate the induction of superoxide production with LPC species 16:0 and 18:1, dihydroethidium (DHE), a dye specific for superoxide was used. Upon fluorescent microscopy inspection, cells that were incubated with LPC 16:0 and LPC 18:1 had higher fluorescent signals than control cells (Figure 10.A). Similar results were obtained by a fluorescence plate reader (Figure 10.B).

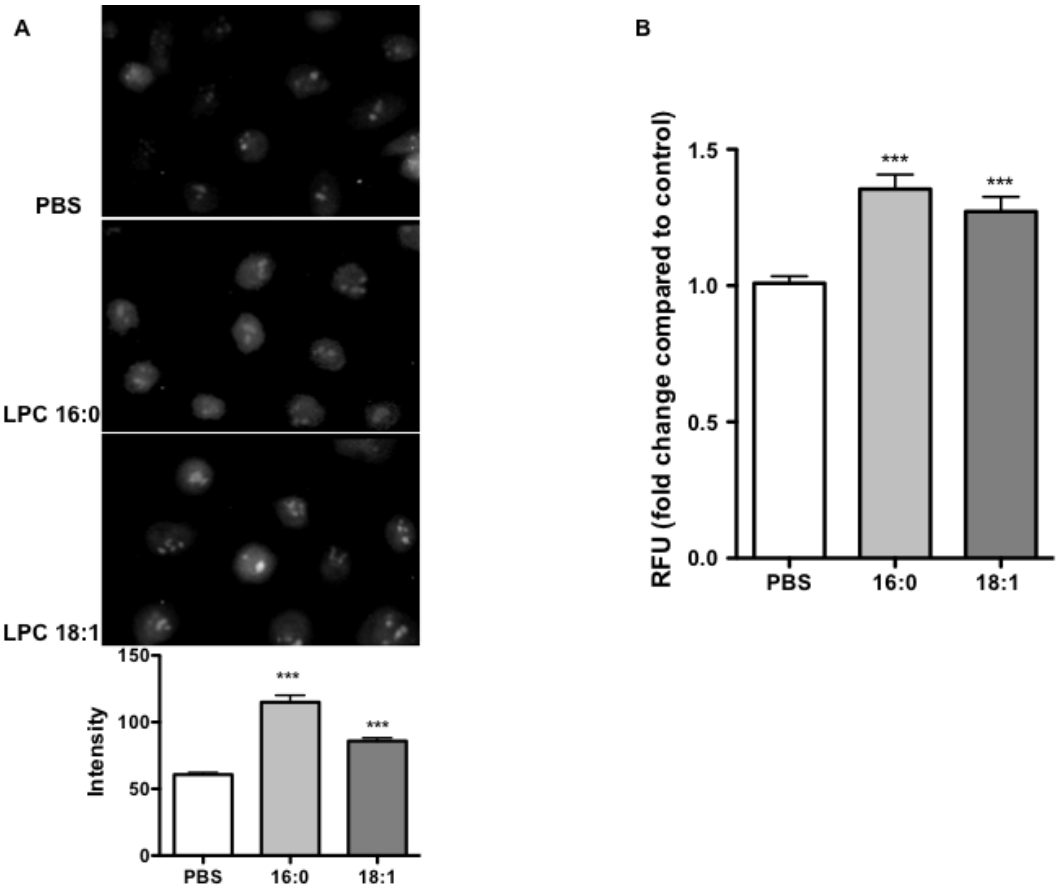

Figure 10. LPC 18:1 and LPC 16:0 induce superoxide production. Cells were grown on a glass coverslip and preincubated with 15 µM DHE in the presence of 20 µM DETCA. Thereafter, cells were exposed to 60 µM LPC 18:1 or PBS in PBS containing 5% FCS for 15 min, followed by fluorescent microscopy (A). Cells plated in 96-well dishes were treated as in (A) followed by fluorometric superoxide quantification (B). Both fluorescent microscopy and plate fluorescent readings showed an increase in superoxide production after treatment of cells with LPC 16:0 or LPC 18:1. Results shown are mean ± SEM, of 3 independent experiments performed in triplicates and analyzed by one-way ANOVA with Tukey's post-hoc test. If otherwise not indicated, asterisks show significance compared to PBS control (***p<0,001).

Localization of ROS in cells treated with LPC 16:0 and 18:1

In order to investigate the distribution of ROS within the cell, confocal microscopy was performed. Cells were transfected with expression plasmids encoding fluorescence-tagged mitochondrial or endoplasmic reticulum (EF) markers and

exposed to LPC 16:0 and LPC 18:1 or PBS. Confocal microscopy revealed that the majority of LPC 16:0-induced ROS co-localized with the mitochondria (Figure 11.B), while ROS induced by LPC 18:1 only partially co-localized with the mitochondria (Figure 11.C). LPC 18:1-induced ROS did not co-localize with ER marker, indicating that ER is not the source of ROS in 18:1 treated cells, however, distinct green spots in the merge image indicate a substantial contribution of cytosolic ROS sources (Figure 11.D).

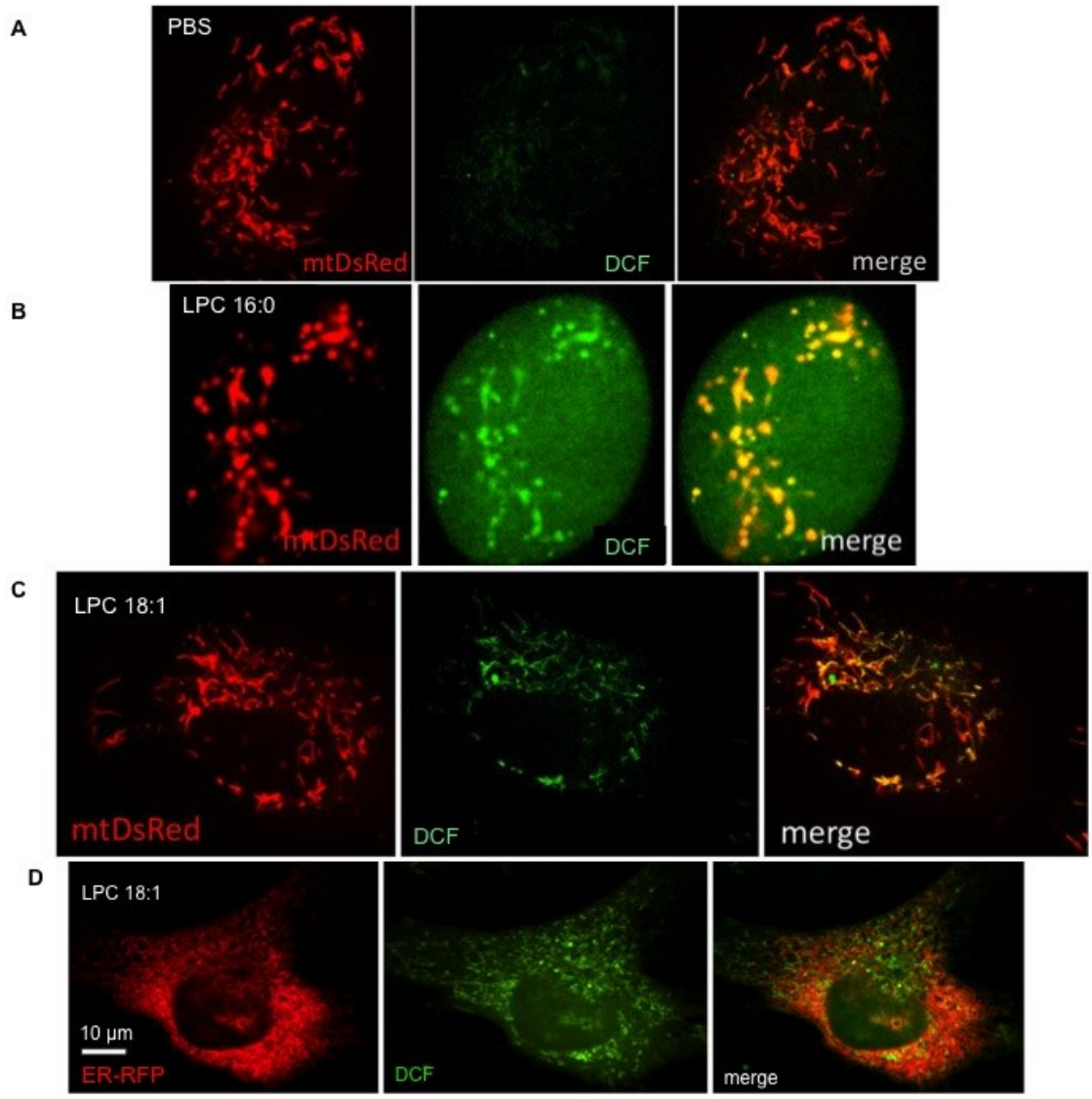

Figure 11. Localization of LPC 16:0- and LPC 18:1- induced intracellular ROS. EA.hy926 cells were transfected with plasmids encoding either ER- or mitochondria-targeted RFP. Twenty four hours after transfection, cells were labeled with H_2DCFDA dye and exposed to 60 µM LPC 16:0 (B), LPC 18:1(C,D) or PBS (A) at 37°C for 15 min. Fluorescence was assessed by confocal microscopy

using mitochondrial- and endoplasmic reticulum-specific RFP marker and a H_2DCFDA ROS marker (green). Co-localization (yellow) was achieved by merging RFP and ROS signals (merge images). Most of LPC 16:0-induced ROS signal co-localized with the mitochondrial signal (B). The LPC 18:1-induced ROS signal partly co-localized with the mitochondrial signal (C), but it did not co-localize with the ER-signal (D) Results are representative images of two experiments performed in triplicates.

LPC 18:1 induces superoxide release in the cell media

To investigate if LPC 18:1 induces release of ROS into the media, Amplex Red assays were performed. Amplex Red added to the cell media detects specifically hydrogen peroxide. When cells were treated only with 10 μM LPC 18:1 or PBS (vehicle), no difference was observed between treatments; however when cells were treated with the LPC or vehicle in the presence of extracellular superoxide dismutase, there was a significant increase in the Amplex Red signal i.e. H_2O_2 in the medium of cells treated with LPC 18:1 compared to vehicle (Figure 12). In order to examine if the source of superoxide is uncoupled eNOS, 100 μM L-NNA was additionally included into incubations. The failure of L-NNA to alter H_2O_2 production, excluded the involvement of eNOS (Figure 12.).

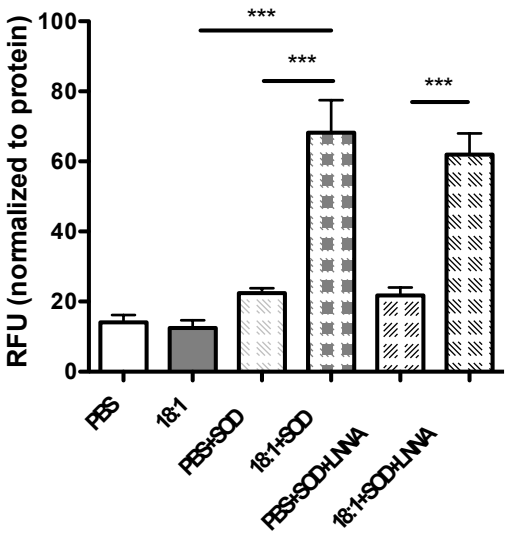

Figure 12. Production of extracellular ROS in cells treated with LPC 18:1. Amplex Red Assay was performed in cells exposed to 10 μM LPC 18:1 or PBS in the presence or absence of PEG-catalase (300 U/ml) or PEG-SOD (75 U/ml) and L-NNA (100μM) in HEPES-buffered Tyrodes solution containing no FCS at 37°C for 15 min. The hydrogen peroxide levels in LPC 18:1-treated cell media, in the absence of PEG-SOD, was not changed, compared to control. In the presence of PEG-SOD, there was a significant increase in the amount of hydrogen peroxide in LPC 18:1-treated cells compared to control. eNOS was not the source of the superoxide (converted to H_2O_2), as L-NNA inhibition had no effect on the H_2O_2 levels. The presented values are catalase-sensitive values obtained by subtraction of values obtained in the presence of catalase from those in the absence of catalase. Results shown are mean ± SEM, of 3 independent experiments performed in triplicates and analyzed by one-way ANOVA with Tukey's post-hoc test. If otherwise not indicated, asterisks show significance compared to PBS control (***p<0,001).

eNOS is not the source of LPC 18:1-induced intracellular superoxide

In order to determine if eNOS is the source of LPC 18:1-induced superoxide, superoxide was measured with DHE fluorescent dye, in the presence or absence of the eNOS inhibitor L-NNA. As shown in Figure 13, L-NNA had no effect on the

produced superoxide, indicating that eNOS is not involved in LPC 18:1 –induced intracellular superoxide production.

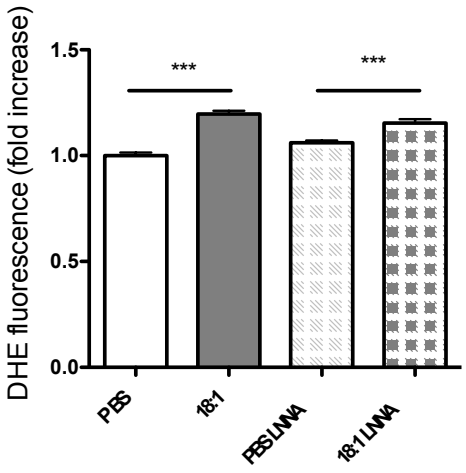

Figure 13. Involvement of eNOS in superoxide production. Cells were plated in 96-well dishes and preincubated with 15 µM DHE in the presence of 20 µM DETCA with or without 100 µM L-NNA. Thereafter, cells were exposed to 60 µM LPC 18:1 or PBS in 5% FCS-containing PBS for 15 min, followed by fluorometric superoxide quantification. Inhibition of eNOS with L-NNA had no effect on superoxide production, indicating no role of eNOS in intracellular superoxide production. Results shown are mean ± SEM, of 3 independent experiments performed in triplicates and analyzed by one-way ANOVA with Tukey's post-hoc test. If otherwise not indicated, asterisks show significance compared to PBS control (***p<0,001).

Tiron improves NO bioavailability in cells treated with LPC 18:1

As LPC 18:1 seems to induce predominantly superoxide production, the superoxide scavenger Tiron was added to the LPC 18:1 treated cells, and nitrite in the medium, as NO indicator, was measured. When the cells treated with LPC 18:1 were co-incubated with 100 µM Tiron, there was a significant improvement in the NO bioavailability, as shown in Figure 14.

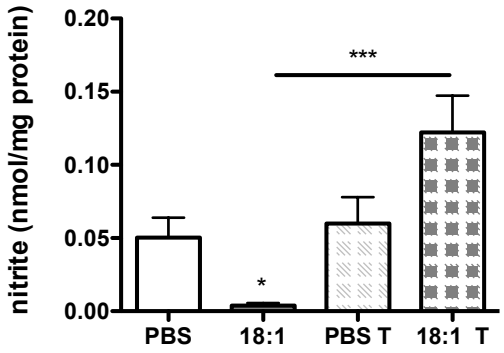

Figure 14. Effect of Tiron on nitrite levels of LPC 18:1-treated cells. Cells were treated with 60 µM LPC 18:1 or vehicle control (PBS) with or without 100 µM eNOS inhibitor L-NNA in the presence or absence of 100 µM superoxide scavenger Tiron in 5% FBS-containing medium for 15 minutes. Thereafter, medium was collected, and protein lysates were used for normalization. Nitrite was measured by HPLC. Tiron recovered the LPC 18:1-induced decrease in nitrite levels. All nitrite values shown are eNOS specific, as nitrite values of incubations done in the presence of L-NNA (eNOS unspecific nitrite) were subtracted from all measurements. Results shown are mean values ± SEM of 3 independent experiments done in sextuplicates, and analyzed by one-way ANOVA with Tukey's post-hoc test. If otherwise not indicated, asterisks show significance compared to PBS control (*p<0,05, **p<0,01, ***p<0,001).

LPC 18:1-induced impaired of vasorelaxation is improved by Tiron

To investigate the functional implication of the decreased NO bioavailability upon LPC 18:1 exposure, wire myography was performed on mouse aortic rings. Rings were incubated with 10 µM LPC 18:1 in PSS buffer without FBS for 15 minutes. As shown in Figure 15, the rings preincubated with LPC 18:1 (line with black squares) showed an impaired acetylcholine (Ach) - induced relaxation compared to PBS treated control rings (line with black circles). However, if the rings were additionally incubated with 100 µM Tiron, the relaxation was improved. This was particularly obvious at the highest Ach- concentrations, where control rings and LPC 18:1-treated rings (+Tiron) exhibited a similar degree of relaxation (line with white squares).

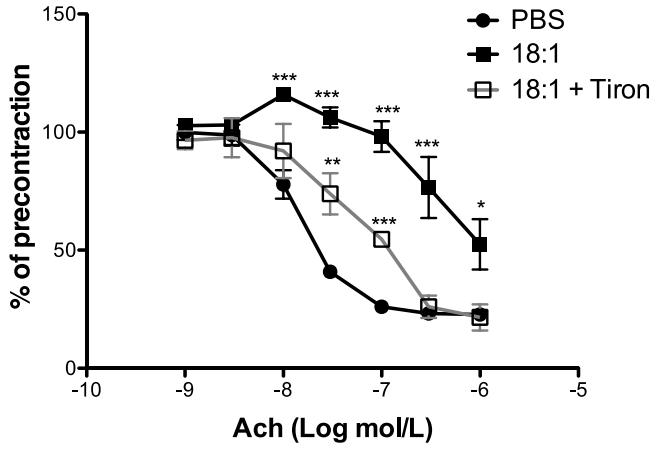

Figure 15. Effect of LPC 18:1 on mouse aortic ring relaxation. Mouse aortic rings (5 for each condition) were incubated with 10 µM LPC 18:1 or PBS for 15 min with or without 100 µM Tiron followed by NE pre-constriction and relaxation to cumulative addition of Ach. Relaxation values were expressed as a percentage of the initial NE-induced contraction. LPC 18:1 caused an impaired relaxation compared to control; however if mouse aortic rings were co-incubated with Tiron, there was no impairment in relaxation with higher concentrations of Ach, compared to control. Results are mean ±SEM of 3 independent experiments and analyzed by two-way ANOVA with Bonferroni post-hoc test. Asterisks show significance compared to PBS control rings (*p<0,05, **p<0,01, ***p<0,001).

Nox1/2 and NOX4 are not involved in LPC 18:1-induced impairment of relaxation in mouse aortic rings

Apocynin, a Nox1/2 inhibitor was used in myography experiments to investigate the potential role of Nox1/2 in LPC 18:1 induced impaired relaxation in mouse aortic rings. However, apocynin showed neither a positive nor a negative effect on mouse aortic ring relaxation after LPC 18:1 exposure (Figure 16.A). Nox4 -/- mice were used to investigate the role of Nox4 in LPC 18:1-induced impaired relaxation of mouse aortic rings. Both wild type and knock out rings showed an impairment of relaxation after LPC treatment, but there was no difference between the two groups (Figure 16.B).

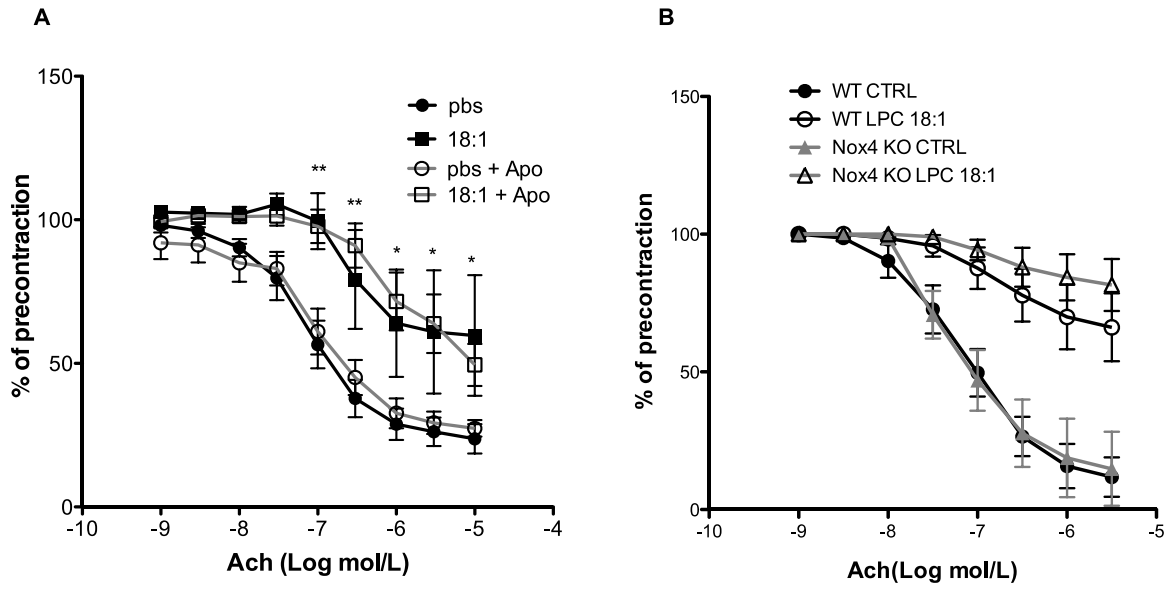

Figure 16. Apocynin and Nox4 had no effect on LPC 18:1 impaired relaxation. A) Mouse aortic rings (5 for each condition) were incubated with 10 μM LPC 18:1 or PBS for 15 min with or without the addition of 100 μM apocynin (Nox1/2 inhibitor) followed by NE preconstriction and relaxation to cumulative addition of Ach. B) Mouse aortic rings from WT and Nox4 KO mice (6 for each condition) were incubated with 10 μM LPC 18:1 or PBS for 15 min followed by NE preconstriction and relaxation to cumulative addition of Ach. Relaxation values were expressed as a percentage of the initial NE-induced contraction. Apocynin had no effect on the LPC 18:1-induced impairment of relaxation. LPC 18:1-induced impairment of relaxation was similar in wild type and Nox4 knock out mice. Results are mean ±SEM of 3 independent experiments and analyzed by two-way ANOVA with Bonferroni post-hoc test. Asterisks show significance compared to PBS control rings (*p<0,05, **p<0,01, ***p<0,001).

LPC 18:1 decreases the NO bioavailability in mouse aortic rings

As LPC 18:1 caused impairment of Ach-induced relaxation in mouse aortic rings, known to rely on stimulation of eNOS and concomitantly increased NO bioavailability, we investigated the impact of LPC 18:1 on the NO bioavailability in mouse aortic rings. The organ bath experiment LPC 18:1 showed a decreased L-NA to NE contraction ratio in the mouse aortic rings treated with LPC 18:1, indicating lower NO availability in LPC 18:1-treated rings, compared with controls

(Figure 17.A). The decreased NO bioavailability in rings exposed to LPC 18:1 was further confirmed by measuring the nitrite levels in incubation buffers of control and LPC 18:1 treated rings. The nitrite levels were significantly lower in rings treated with LPC 18:1 compared to control rings (Figure 17.B).

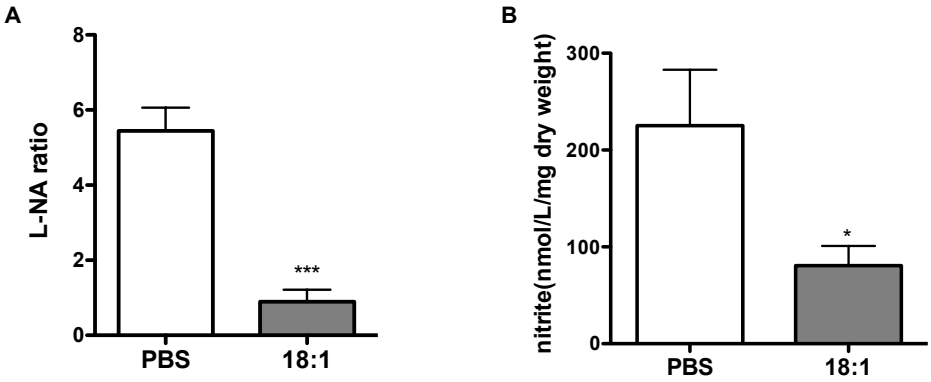

Figure 17. Bioavailability of NO in mouse aortic rings exposed to LPC 18:1. Mouse aortic rings were treated with 10 μM LPC 18:1 or PBS for 15 min and preconstricted with phenylephrine to 10% of maximal contraction followed by addition of 300 μM L-NA (eNOS inhibitor) (A). The result shows ratio (L-NA ratio) of constriction achieved after and before addition of L-NA. B) Mouse aortic rings were treated with LPC 18:1 in 96 well dishes (one ring per well) after which incubation buffer was collected for nitrite measurement. Both the functional assay (A) and nitrite quantification (B) show a lower NO bioavailability in rings treated with LPC 18:1 compared with control. Results are mean ±SEM of 3 independent experiments done in triplicate and analyzed by unpaired t-test (*p<0,05, **p<0,01, ***p<0,001).

Superoxide levels are slightly but not significantly increased in mouse aortic rings exposed to LPC 18:1

Superoxide levels were measured with DHE dye to investigate whether LPC 18:1 increases the superoxide levels in mouse aortic rings. Although there was a tendency towards a higher superoxide levels in LPC 18:1 treated rings, it did not reach statistical significance (Figure 18).

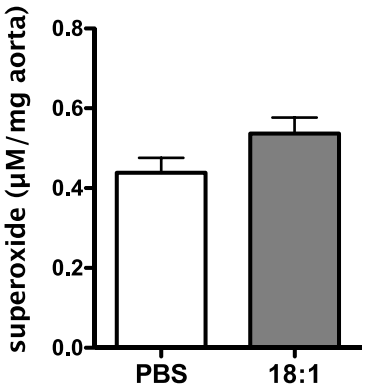

Figure 18. Superoxide levels in LPC 18:1 treated mouse aortic rings. Rings were incubated with or without 10 µM LPC for 15 minutes followed by 30 minutes of DHE (10 µM) in 37°C. DHE products were extracted from the aortic rings and used for HPLC measurement. There was no significant difference between control and LPC 18:1-treated mouse aortic rings. Results are mean ±SEM of 3 independent experiments done in triplicate and analyzed by unpaired t-test.

Impact of LPC concentration and FBS on LPC 18:1 bioactivity

As some experiments required the absence of FBS for technical reasons, 10 µM LPC concentration was used, based on established protocols from previous studies performed in our group (20). In order to compare the bioactivity of the two applied LPC concentrations under different experimental conditions, namely in the absence or presence of 5% FBS, the impact 10 µM LPC without FBS and of 60 µM LPC with 5% FBS on ROS and nitrite was studied in EA.hy926 cell line. Under both experimental conditions LPC 18:1 caused a similar decrease in nitrite levels (Figure 19.A) and s similar increase in ROS levels (Figure 19.B). These findings indicate that the bioactivity of LPC 18:1 under both applied experimental conditions was similar.

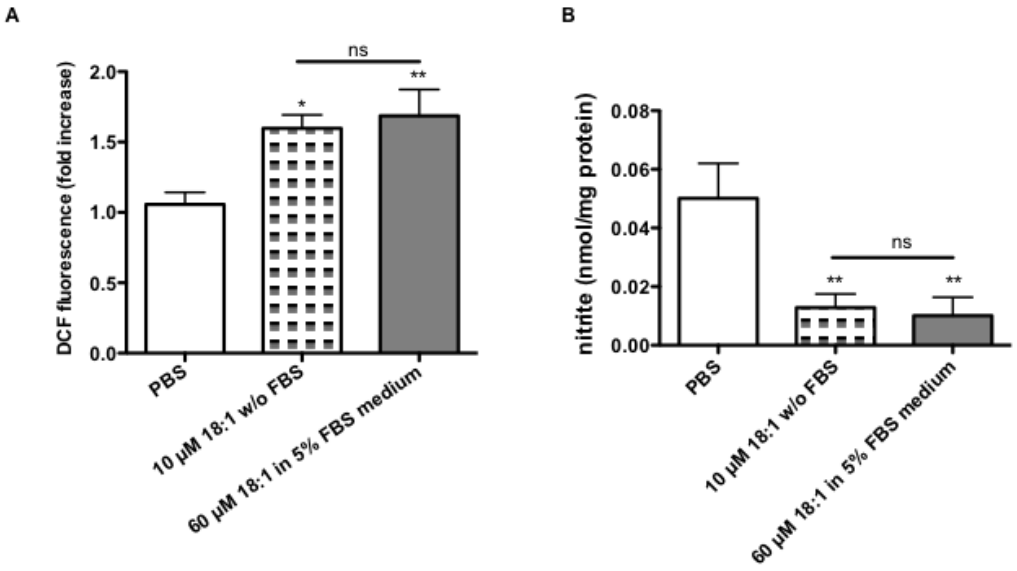

Figure 19. Comparison of effects of 10 µM LPC 18:1 without FBS and 60 µM LPC 18:1 with 5% FCS. A) EA.hy926 cells were preincubated with or without 100 µM L-NNA (eNOS inhibitor), after which they were exposed to vehicle control (PBS), 10 µM LPC 18:1 in medium without LPC or 60 µM LPC 18:1 in medium with 5% FBS for 15 minutes. Thereafter, medium was collected, and protein lysates were used for normalization. B) Cells were preincubated with 10µM H_2DCFDA fluorescent dye, after which they were treated with 60 µM LPC 18:1 in 5% FBS medium, 10 µM LPC 18:1 in medium without FBS or vehicle control (PBS) for 15 minutes. Thereafter, cells were lysed and fluorescence was measured. Both 10 and 60 µM LPC 18:1 decreased the nitrite levels, compared to control, but there was no difference between the two LPC treatments (A). Both LPC 18:1 concentrations induced intracellular ROS levels, compared to control, but there was no significant difference between the two LPC treatments (B). Results shown are mean ± SEM, of 3 independent experiments performed in sextuplicates (A)/triplicates (B) and analyzed by one-way ANOVA with Tukey's post-hoc test. If otherwise not indicated, asterisks show significance compared to PBS control (*p<0,05, **p<0,01,ns - not significant).

DISCUSSION

Previous work from our laboratory provided evidence that these LPC cause impairment in endothelium-dependent vasorelaxation of mouse aortic rings (24). While induction of proconstricting prostanoids was found to play a pivotal role in the impairment of relaxation caused by LPC 18:2 and 20:4, the cause of attenuated relaxation observed in rings exposed to LPC 16:0 and 18:1 remained undiscovered. eNOS plays a crucial role in vasorelaxation, due to the production of NO that, by promoting the intracellular cGMP levels, relaxes underlying smooth muscle cells (45). Therefore, the present study aimed at examining whether and how LPC species 16:0, 18:1, 18:2 and 20:4 affect eNOS and NO bioavailability in vascular endothelium.

Effect of LPC species on eNOS and NO bioavailability

We exposed the EA.hy926 cells to 60 μM LPC species in 5% FBS-containing media for 15 minutes or 1 hour. Concentrations of LPC used were not physiological, as 60 μM LPC in 5% serum corresponds to 1,2 mM LPC in full serum, similar to conditions in hyperlipidemic subjects were LPC concentrations reach milimolar levels (91) (as reference, physiological concentrations of total LPC found in plasma were around 190 μM (8)). The concentrations used were not cytotoxic as shown with MTT test.

In order to examine if acute pathophysiological concentrations of LPC species 16:0, 18:1, 18:2 and 20:4 change the phosphorylation of eNOS, thereby possibly modulating the production of NO, we investigated by Western blotting the changes in activating phosphorylation on Ser1177 compared to total eNOS protein. Neither the 15-minute nor the 1-hour exposure to LPC species altered the Ser1177 phosphorylation of eNOS. Some studies have shown a change in total eNOS protein after exposure to LPC 16:0 (80, 81), but the concentrations of LPC 16:0 used were higher than in our experiments, and the exposure time was longer (2h and 12h, respectively). It has also been shown that LPC 16:0 does not change the basal phosphorylation of eNOS, but upon activation of eNOS with histamine the phosphorylation induction in LPC 16:0 treated cells is reduced compared to control

(83, 92). However, to the best of our knowledge, no literature is available on the effect of unsaturated LPC on eNOS phosphorylation so far.

Although there was no change in phosphorylation of eNOS upon exposure of cells to LPC, we examined whether the treatment of cells with LPC affects the NO bioavailability, as described previously for LPC 16:0 (82, 93). We therefore measured the nitrite levels in cell media after treatment with LPC species. Nitrite, the end product of NO metabolism, was used to assess the NO production, as previously published (24, 73, 94). After a 15-minute exposure, LPC 18:1 caused a statistically significant decrease in nitrite levels compared to control. LPC 16:0 and LPC 20:4 showed a tendency towards a decrease, but it was not significant. After a 1-hour exposure, none of the LPC species showed a statistically significant change in nitrite levels. Contrary to our results, Konopatskaya et al. (82) showed that exposure of HUVEC cells to 20 μM LPC 16:0 (no FBS) for 15 minutes caused a NO-specific increase in cGMP, indicating the increase in NO bioavailability. In contrast, Jia et al. (93) found decreased NO levels after exposure of HUVEC cells to LPC 16:0 for 24h. Although previous publications showed that 24h treatment with LPC 16:0 can cause ADMA formation, that blocks NO production (93), this is most likely not the case in our study due to a very short incubation period with the LPC species.

Because we found no changes in phosphorylation, but decreased nitrite levels, we investigated whether LPC affected the ratio between the active dimer form and monomeric form of eNOS, to see if the activity was changed upon exposure to LPC. LPC 16:0 and 18:1 caused a small, but significant decrease in the dimer to monomer ratio after a 15 minute exposure, whereas LPC 16:0, 18:1 and 18:2 caused a decrease in dimer to monomer ratio after an 1 hour exposure. To further examine the relationship between alterations in dimer to monomer ratio and eNOS activity, the eNOS activity assay was done. In contrast to decreased dimer to monomer ratio, there was no significant decrease in eNOS activity, indicating that the small decrease of the active dimer form of eNOS was not the cause of a decreased nitrite level in the cell media.

Effect of LPC species on ROS production

It is well known that LPC 16:0 is a potent inducer of ROS (80, 93, 95, 96). Based on this fact, together with the capacity of ROS to scavenge and inactivate NO, we examined whether, in our experimental conditions, LPC 16:0 as well as the three unsaturated LPC species induce ROS, and whether LPC-induced ROS impacts NO bioavailability. We used H_2DCFDA fluorescent dye that measures all intracellular ROS (97); primarily peroxides, peroxynitrite and marginally superoxide.

LPC 16:0 was a more potent inducer of ROS than LPC 18:1 after 15 minutes of incubation. Previous reports also showed that LPC 16:0 induces ROS production in endothelial cells (80, 96, 98), but little is known about LPC 18:1. One publication describes that LPC 18:1 has no effect on ROS induction in RAW 264.7 cells (99), while another shows that LPC 18:1 inhibits neutrophil superoxide production, but only if prepared in an organic solution (100).

After 1 hour of incubation none of the LPC induced an increase of intracellular ROS, however LPC 18:2 and LPC 20:4 caused a decrease in ROS comparable to that of cells treated with DETCA, the inhibitor of superoxide dismutase. DETCA alone caused a decrease in the fluorescence signal, in line with a low sensitivity of the H2DCFDA dye for superoxide. The observed decrease in ROS upon exposure of cells to LPC 18:2 or 20:4 may reflect a) an inhibitory role of these LPC species on intracellular ROS production; b) inhibition of the superoxide dismutase (similar to DETCA) or c) an induction of the activity of catalase, resulting in a repaid conversion of peroxide to water. However, we can only speculate, as no additional experiments were done to further investigate the action of these two LPC. Little is known about the effect of LPC 18:2 and 20:4 on ROS in endothelial cells; a study showed (99) that these LPC cause an increase in ROS production in RAW 264.7 macrophages (10 minutes exposure to 20 μM LPC without the presence of FBS).

As LPC 18:2 and 20:4 neither decreased nitrite levels significantly nor increased intracellular ROS production, we focused on LPC 16:0 and 18:1 to further elucidate the source and type of ROS produced in the EA.hy 926 cells upon 15 minutes exposure to these LPC.

NADPH oxidases are an important source of ROS in endothelial cells (48), and in EA.hy 926 cells predominantly Nox4 and Nox1/2 are expressed (101). We used Nox4 and Nox1/2 inhibitors to investigate their involvement in LPC-induced ROS formation. Nox1/2 inhibitor apocynin had no effect on ROS formation; however the Nox4 inhibitor VAS2870 completely abolished both LPC 16:0- and 18:1 - induced ROS indicating an involvement of Nox4 in ROS formation. This is in line with previously published work from Heinloth et al. (95) where the authors showed that the source of LPC 16:0- induced ROS in HUVEC is NADPH oxidase, but they did not specify the isoform of the oxidase. Heumüller et al (102) reported however, that apocynin is not active in endothelial cells, and is not suitable as a Nox1/2 inhibitor. Accordingly, we cannot exclude the involvement of Nox1/2 in LPC-induced ROS production.

Uncoupled eNOS, xanthine oxidase and COX are also potential sources of ROS in endothelial cells (48, 103). Therefore, cells were incubated with L-NNA, allopurinol and indomethacin, respectively, to examine the role of these enzymes in the LPC-induced ROS.

Inhibition of eNOS resulted in attenuation of LPC 18:1-induced ROS formation. This, together with decreased eNOS dimer to monomer ratio strongly indicates that, uncoupled eNOS contributes to increased levels of ROS in LPC 18:1 treated cells. In contrast, however, there was no impact of eNOS inhibition on LPC 16:0 – induced ROS, arguing against eNOS as a source of ROS upon exposure of cells to LPC 16:0. Since allopurinol decreased both basal and LPC-induced ROS, it seems that xanthine oxidase does not contribute significantly to LPC-induced ROS formation. In contrast, the inhibition of COS by indomethacin decreased both LPC 16:0- and LPC 18:1-induced ROS. However, due to the fact that indomethacin alone exhibits antioxidative and ROS scavenging activities (104), experiments with COX inhibitors other than indomethacin should clarify the contribution of COX enzymes to LPC-induced ROS.

The fact that inhibition of eNOS, xanthine oxidase, COX and NADPH oxidase can inhibit LPC 18:1-induced ROS, is very interesting, indicating that LPC 18:1-induced ROS is generated by various cellular enzymatic sources. Ray and Shah (48) proposed a hypothesis by which superoxide generated by NADPH oxidase can modify the ROS production of other enzymes. NADPH generated superoxide can cause eNOS uncoupling, leading to the production of superoxide instead of

NO. Furthermore, xanthine dehydrogenase, through oxidation by superoxide is converted to xanthine oxidase, which may result in an increased superoxide production. In contrast to LPC 18:1-induced ROS, the LPC 16:0 - induced ROS seems to come predominantly from one source, mainly NADPH oxidase, as only inhibition of Nox4 could completely inhibit the ROS signal.

Experiments with Tiron, a superoxide scavenger and DETCA, a SOD inhibitor, showed that LPC 16:0 induced ROS signal obtained with H_2DCFDA dye cannot be abolished completely with a superoxide scavenger or a SOD inhibitor, indicating that only one part of the induced ROS is superoxide, and the rest are other species of ROS, presumably hydrogen peroxide, most likely produced directly by Nox4 (57). Contrary to LPC 16:0, LPC 18:1-induced ROS signal could be completely abolished with both Tiron and DETCA, indicating that LPC 18:1 induces exclusively production of superoxide.

To confirm this hypothesis, we measured superoxide production with DHE fluorescent dye, specific for superoxide. Both fluorescent microscopy and experiments done with a fluorescence plate reader showed that both LPC 16:0 and LPC 18:1 induce superoxide production The less pronounced difference in the magnitude of superoxide induction between the two LPC, compared with the much more pronounced difference in the total intracellular ROS production, in favor of LPC 16:0, argues for the production of LPC 16:0-induced superoxide and non-superoxide ROS.

Our findings regarding LPC 16:0-induced ROS are in line with several previous studies showing LPC 16:0 induced superoxide production in endothelial cells (95, 96). In contrast, however, nothing is known for LPC 18:1.

To investigate the potential differences in localization between LPC 16:0- and LPC 18:1- induced ROS, cells were transfected with mitochondrial and ER labeled markers. Cells treated with LPC 16:0 had ROS signals almost completely co-localized with the mitochondrial signal. This is in line with a previously published work of Watanabe et al. (96), which showed that LPC 16:0 induces mitochondrial ROS in HUVEC.

The LPC 16:0-treated cells, compared to control and 18:1-treated cells, were also more rounded in morphology. The reason for the changed morphology is still unclear, as MTT test showed no cytotoxicity of the 60 μM LPC 16:0. As LPC 16:0 could act as a detergent, it is possible that it causes a change in membrane

stability following its incorporation (105) causing a change in the adherence of the cells.

Cells treated with LPC 18:1 had ROS signals partially co-localized with the mitochondrial signal, while a part was most probably in the cytoplasm, since it did not co-localize with the ER signal. Cytoplasmic localization of LPC 18:1-induced ROS is likely considering pronounced relative contribution of various cellular enzymes localized in cytosol to LPC 18:1-induced ROS formation.

The capacity of pharmacological Nox4-inhibition to attenuate LPC 16:0-induced ROS and predominant, almost exclusive localization of LPC 16:0-induced ROS in mitochondria is discrepant considering previously described intracellular membrane localization of Nox4 (106), as well as localization in the nucleus (107). A possible explanation for this might be mitochondrial localization of Nox4. It has been shown for cardiomyocytes (108) that Nox4 is located in the mitochondria, but so far this was not found in the endothelial cells. Another possible explanation might be triggering of a massive mitochondrial ROS production by minute amounts of LPC 16:0-induced, Nox4-generated ROS, not detectable in cytosol by fluorescence microscopy.

The difference in the ROS localization and generated types of ROS species might explain the difference in the bioactivity between LPC 16:0- and LPC 18:1- induced ROS. More specifically, the higher amounts of ROS generated by LPC 16:0 exert less NO inactivating capacity and/or their spatial distribution within cells hampered their interaction with NO.

This is in contrast to a pronounced NO inactivating capacity of rather low amounts of LPC 18:1-induce ROS, most likely generated in a close proximity to the sites of NOS production. Since we found in addition to intracellular also extracellular superoxide formation, we examined whether uncoupled eNOS, localized near plasma membrane (82), could be a source of extracellular superoxide. Inhibition of eNOS with L-NNA had no effect on the H_2O_2 levels measured in media in the presence PEG-SOD, indicating that eNOS is not the source of extracellular superoxide. We also investigated if eNOS was the source of intracellular superoxide, but experiments with L-NNA showed that it was not the case. Considering cell membrane localization of Nox1/2, they could potentially be the source of the extracellular superoxide. Since apocynin is not a reliable inhibitor in

endothelial cells (102), other approaches, such as siRNA silencing, should be used to test this hypothesis.

Since we found initially that inhibition of eNOS by L-NNA attenuates LPC 18:1-induced intracellular ROS measured by H_2DCFDA, we also investigated by employing DHE, a superoxide specific dye, if eNOS acts as the source of intracellular superoxide in LPC 18:1-treated cells. Interestingly, inhibition of eNOS had no impact on intracellular LPC 18:1-induced superoxide formation.

This is in a sharp contrast to what was found with H_2DCFDA, implying that eNOS contributes to LPC 18:1-induced ROS most probably by providing NO for peroxynitrite and not by provision of superoxide.

Since Tiron used in ROS measurements completely abolished the LPC 18:1 –induced ROS production, we examined if Tiron could counteract the detrimental effect of LPC 18:1-induced ROS on nitrite. Improved NO bioavailability by Tiron confirmed that the LPC 18:1-induced superoxide scavenges the NO produced by the cells, thereby decreasing the NO bioavailability.

To confirm cell culture results, experiments were also done in mouse aortic rings. As FBS is not suitable for wire myography experiments, LPC 18:1 was used in the concentration of 10 µmol/L without the presence of FBS. This concentration was previously published as nontoxic both for cells and mouse aortic rings (20, 24).

As previously published (24), LPC 18:1 impaired endothelium –dependent relaxation, but the relaxation could be ameliorated when Tiron was added to the rings along with the LPC 18:1, indicating that superoxide production was induced with LPC 18:1 treatment.

We therefore measured superoxide levels in the rings, but unlike in the cell culture experiments where LPC 18:1 induced significant superoxide production, the superoxide levels in LPC-treated mouse aortic rings showed a tendency to be increased, but did not reach statistical significance. The protocols by which superoxide was measured and the material (tissue vs. cells) were different, possibly explaining the difference in the results.

NO bioavailability in mouse aortic rings was significantly decreased, similar to cell culture data. This, along with the fact that Tiron ameliorated the acetylcholine relaxation, indicates that superoxide induced by LPC 18:1 reacts promptly with NO leading to production of peroxynitrite, leading in turn to impaired relaxation.

We investigated if Nox1/2 or Nox4 were involved in the impairment of endothelium-dependent relaxation after LPC treatment. Nox1/2 was inhibited with apocynin that showed no impact on aortic ring relaxation. Again, because of the fact that that apocynin is not possibly sufficiently active in the vascular tissue (102), we cannot rule out the possibility that Nox1/2 is involved in this effect of LPC 18:1. By using Nox4 knock out mice, we could clearly demonstrate that Nox4 is not involved in LPC 18:1-induced impairment of relaxation.
Although some results were not comparable to the ones observed in cell culture experiments, we could still show that acute exposure to LPC 18:1 has a detrimental effect on NO bioavailability in mouse aortic rings.

To clarify whether 10 µM LPC concentration without FBS has a different effect than 60 µM with FBS due to binding to albumin and other serum proteins and lipoproteins (91, 105), we performed cell culture experiments under both conditions. We found that both LPC 18:1 concentrations induced intracellular ROS and decreased nitrite levels to a similar extent, thus validating the results achieved in mouse aortic ring experiments.
The critical micellar concentration (CMC) has been calculated for LPC 16:0, and it ranges from 7-30 µM, depending on the preparation (8, 100). The addition of a double bond to a saturated acyl chain decreases hydrophobicity nearly equally as the removal of two methylene units, thus the CMC of LPC 18:1 should be similar to that of LPC 16:0 (8). It has been shown that the preparation of LPC is very important for LPC action (100), where LPC 16:0 and LPC 18:1 showed an inhibitory effect on superoxide production in human neutrophils if dissolved in ethanol, but enhanced superoxide production if dissolved in an aqueous solution. The proposed mechanism was the formation of micelles in the aqueous solutions that then had a detrimental effect.
As our 10 µM LPC 18:1 was prepared in PBS, it is therefore possible that LPC 18:1 formed micelles that caused ROS production, and consequentially a decreased NO bioavailability. The 60 µM LPC 18:1 was also prepared in PBS, permitting formation of micelles. Because it was later mixed with a 5% FBS-containing medium prior to application onto cells, some of the LPC molecules might have bound to bovine serum albumin (4), while some might have remained in the micellar form, allowing them to affect cells as 10 µM LPC 18:1 without FBS.

To study at which concentration the LPC 18:1 induces the effects seen on intracellular ROS and nitrite levels, we performed additional concentration dependent experiments (10, 30, 60 and 120 μM LPC 18:1) using 5% FBS conditions (see Appendix).

As expected, the lower concentrations of LPC 18:1 (10 and 30 μM) did not induce intracellular ROS formation, while 120 μM of LPC induced ROS production, but not significantly higher compared to 60 μM LPC 18:1 (Suppl. figure 1. A). To our surprise, 10 and 30 μM LPC 18:1 concentrations decreased the nitrite levels to the same extent that were achieved with 60 μM LPC, while nitrite levels were not altered by 120 μM LPC 18:1 (Suppl. figure 1. B).

The decrease in the nitrite levels with 10 and 30 μM is therefore not a consequence of induced ROS production, but of other mechanism(s). We can only speculate the mechanism behind this effect. The physiological concentration of LPC 18:1 is about 25 μM, as it comprises 11-13 % of total 190 μM LPC found in plasma (8, 109). 10 and 30 μM LPC 18:1 in 5% FBS corresponds to 200 and 600 μM in full serum, respectively, making the concentrations higher than physiological. Because one molecule of BSA has been reported to bind 5 molecules of LPC (105), it is possible that with these lower LPC concentrations, most of the LPC molecules are bound to albumin and there is no micellar form of LPC, but rather only LPC in its free form. This might conceivably explain the lack of effect on ROS production of the lower 10 and 30 μM LPC concentrations compared with 60 and 120 μM LPC 18:1.

LPC can integrate into the outer leaflet of the plasma membrane, but because of its polar headgroup it flips less readily to the inner membrane leaflet and the process of flipping can last more than 10h (110). Therefore a direct interaction with eNOS is not likely. Since eNOS is found in caveolae, bound to caveolin-1 that inactivates it, and eNOS becomes active only upon displacement of caveolin-1 with hsp90 and calmodulin, we can only speculate that binding of LPC to the outer leaflet of the membrane changes the local characteristics of the lipid layer, resulting in altered interaction of caveolin-1 with eNOS. Augmentation of the interaction between caveolin-1 and eNOS would attenuate eNOS activity and decrease NO bioavailability.

Another mechanism of eNOS inactivation would be phosphorylation trough protein kinases (111), where LPC binding to a receptor would activate a signaling cascade leading to the phosphorylation. It has been proposed previously (112, 113) that LPC can interact with G protein coupled receptors, namely G2A and GPR4, but due to the fact that the publications were formally retracted, no proven receptors for LPC are known (8).

120 μM LPC was not tested for cytotoxicity by MTT test (LDH assay was done, but due to the high background values of FBS containing media, it was impossible to measure the contribution of cellular LDH). It is possible that this concentration was cytotoxic, and had a dual effect on cells. One effect, similar to 60 μM LPC, is the increase in ROS levels, leading to NO scavenging and decreased NO bioavailability. The second effect, rely upon detergent like properties, with a consequent release the intracellular nitrite, making the overall nitrite readout unchanged compared to control.

Conclusion

Based on our results, LPC 18:1 emerges as an important modulator of NO bioavailability in cells and mouse aortic rings, suggesting its role in human vascular pathobiology in subjects with hyperlipidemia.

BIBLIOGRAPHY

1. Matsumoto T, Kobayashi T, Kamata K. Role of lysophosphatidylcholine (LPC) in atherosclerosis. Current medicinal chemistry. 2007;14(30):3209-20. Epub 2008/01/29.

2. Fuchs B, Muller K, Paasch U, Schiller J. Lysophospholipids: potential markers of diseases and infertility? Mini reviews in medicinal chemistry. 2012;12(1):74-86. Epub 2011/11/11.

3. Larsson KS, K.; Tiberg, F. Lipids: Structure, Physical Properties and Functionality. 1st ed ed. Bridgwater: The Oily Press Lipid Library; 2006.

4. Schmitz G, Ruebsaamen K. Metabolism and atherogenic disease association of lysophosphatidylcholine. Atherosclerosis. 2010;208(1):10-8. Epub 2009/07/03.

5. Kohno M, Yasunari K, Maeda K, Kano H, Minami M, Hanehira T, et al. Effects of cardiac natriuretic peptides on oxidized low-density lipoprotein- and lysophosphatidylcholine-induced human mesangial cell migration. Hypertension. 2000;35(4):971-7. Epub 2000/04/25.

6. Kugiyama K, Sakamoto T, Misumi I, Sugiyama S, Ohgushi M, Ogawa H, et al. Transferable lipids in oxidized low-density lipoprotein stimulate plasminogen activator inhibitor-1 and inhibit tissue-type plasminogen activator release from endothelial cells. Circulation research. 1993;73(2):335-43. Epub 1993/08/01.

7. Vuong TD, de Kimpe S, de Roos R, Rabelink TJ, Koomans HA, Joles JA. Albumin restores lysophosphatidylcholine-induced inhibition of vasodilation in rat aorta. Kidney international. 2001;60(3):1088-96. Epub 2001/09/05.

8. Ojala PJ, Hirvonen TE, Hermansson M, Somerharju P, Parkkinen J. Acyl chain-dependent effect of lysophosphatidylcholine on human neutrophils. Journal of leukocyte biology. 2007;82(6):1501-9.

9. Okita M, Gaudette DC, Mills GB, Holub BJ. Elevated levels and altered fatty acid composition of plasma lysophosphatidylcholine(lysoPC) in ovarian cancer patients. International journal of cancer Journal international du cancer. 1997;71(1):31-4. Epub 1997/03/28.

10. Chen L, Liang B, Froese DE, Liu S, Wong JT, Tran K, et al. Oxidative modification of low density lipoprotein in normal and hyperlipidemic patients: effect of lysophosphatidylcholine composition on vascular relaxation. Journal of lipid research. 1997;38(3):546-53.

11. Kougias P, Chai H, Lin PH, Lumsden AB, Yao Q, Chen C. Lysophosphatidylcholine and secretory phospholipase A2 in vascular disease: mediators of endothelial dysfunction and atherosclerosis. Medical science monitor : international medical journal of experimental and clinical research. 2006;12(1):RA5-16. Epub 2005/12/22.

12. McHowat J, Corr PB. Thrombin-induced release of lysophosphatidylcholine from endothelial cells. The Journal of biological chemistry. 1993;268(21):15605-10. Epub 1993/07/25.

13. Subbaiah PV, Liu M. Comparative studies on the substrate specificity of lecithin:cholesterol acyltransferase towards the molecular species of phosphatidylcholine in the plasma of 14 vertebrates. Journal of lipid research. 1996;37(1):113-22. Epub 1996/01/01.

14. Gauster M, Rechberger G, Sovic A, Horl G, Steyrer E, Sattler W, et al. Endothelial lipase releases saturated and unsaturated fatty acids of high density lipoprotein phosphatidylcholine. Journal of lipid research. 2005;46(7):1517-25.

15. Santamarina-Fojo S, Gonzalez-Navarro H, Freeman L, Wagner E, Nong Z. Hepatic lipase, lipoprotein metabolism, and atherogenesis. Arteriosclerosis, thrombosis, and vascular biology. 2004;24(10):1750-4. Epub 2004/07/31.

16. Zhao Z, Xiao Y, Elson P, Tan H, Plummer SJ, Berk M, et al. Plasma lysophosphatidylcholine levels: potential biomarkers for colorectal cancer. Journal of clinical oncology : official journal of the American Society of Clinical Oncology. 2007;25(19):2696-701. Epub 2007/07/03.

17. Kume N, Cybulsky MI, Gimbrone MA, Jr. Lysophosphatidylcholine, a component of atherogenic lipoproteins, induces mononuclear leukocyte adhesion molecules in cultured human and rabbit arterial endothelial cells. The Journal of clinical investigation. 1992;90(3):1138-44. Epub 1992/09/11.

18. Takahara N, Kashiwagi A, Maegawa H, Shigeta Y. Lysophosphatidylcholine stimulates the expression and production of MCP-1 by human vascular endothelial cells. Metabolism: clinical and experimental. 1996;45(5):559-64. Epub 1996/05/01.

19. Brkic L, Riederer M, Graier WF, Malli R, Frank S. Acyl chain-dependent effect of lysophosphatidylcholine on cyclooxygenase (COX)-2 expression in endothelial cells. Atherosclerosis. 2012;224(2):348-54. Epub 2012/08/21.

20. Riederer M, Lechleitner M, Hrzenjak A, Koefeler H, Desoye G, Heinemann A, et al. Endothelial lipase (EL) and EL-generated lysophosphatidylcholines promote IL-8 expression in endothelial cells. Atherosclerosis. 2011;214(2):338-44.

21. Kohno M, Yokokawa K, Yasunari K, Minami M, Kano H, Hanehira T, et al. Induction by lysophosphatidylcholine, a major phospholipid component of atherogenic lipoproteins, of human coronary artery smooth muscle cell migration. Circulation. 1998;98(4):353-9. Epub 1998/08/26.

22. Cowan CL, Steffen RP. Lysophosphatidylcholine inhibits relaxation of rabbit abdominal aorta mediated by endothelium-derived nitric oxide and endothelium-

derived hyperpolarizing factor independent of protein kinase C activation. Arteriosclerosis, thrombosis, and vascular biology. 1995;15(12):2290-7. Epub 1995/12/01.

23. Froese DE, McMaster J, Man RY, Choy PC, Kroeger EA. Inhibition of endothelium-dependent vascular relaxation by lysophosphatidylcholine: impact of lysophosphatidylcholine on mechanisms involving endothelium-derived nitric oxide and endothelium derived hyperpolarizing factor. Mol Cell Biochem. 1999;197(1-2):1-6. Epub 1999/09/15.

24. Rao SP, Riederer M, Lechleitner M, Hermansson M, Desoye G, Hallstrom S, et al. Acyl chain-dependent effect of lysophosphatidylcholine on endothelium-dependent vasorelaxation. PloS one. 2013;8(5):e65155.

25. Rajendran P, Rengarajan T, Thangavel J, Nishigaki Y, Sakthisekaran D, Sethi G, et al. The vascular endothelium and human diseases. International journal of biological sciences. 2013;9(10):1057-69. Epub 2013/11/20.

26. Galley HF, Webster NR. Physiology of the endothelium. British journal of anaesthesia. 2004;93(1):105-13. Epub 2004/05/04.

27. Verhamme P, Hoylaerts MF. The pivotal role of the endothelium in haemostasis and thrombosis. Acta clinica Belgica. 2006;61(5):213-9. Epub 2007/01/24.

28. Vane JR, Anggard EE, Botting RM. Regulatory functions of the vascular endothelium. The New England journal of medicine. 1990;323(1):27-36. Epub 1990/07/05.

29. Wagner DD, Frenette PS. The vessel wall and its interactions. Blood. 2008;111(11):5271-81. Epub 2008/05/27.

30. Vanhoutte PM. Endothelial dysfunction: the first step toward coronary arteriosclerosis. Circulation journal : official journal of the Japanese Circulation Society. 2009;73(4):595-601. Epub 2009/02/20.

31. Muller WA. Leukocyte-endothelial-cell interactions in leukocyte transmigration and the inflammatory response. Trends in immunology. 2003;24(6):327-34. Epub 2003/06/18.

32. Forstermann U, Sessa WC. Nitric oxide synthases: regulation and function. European heart journal. 2012;33(7):829-37, 37a-37d.

33. Rochette L, Lorin J, Zeller M, Guilland JC, Lorgis L, Cottin Y, et al. Nitric oxide synthase inhibition and oxidative stress in cardiovascular diseases: possible therapeutic targets? Pharmacology & therapeutics. 2013;140(3):239-57. Epub 2013/07/19.

34. Bucci M, Gratton JP, Rudic RD, Acevedo L, Roviezzo F, Cirino G, et al. In vivo delivery of the caveolin-1 scaffolding domain inhibits nitric oxide synthesis and reduces inflammation. Nature medicine. 2000;6(12):1362-7. Epub 2000/12/02.

35. Gratton JP, Fontana J, O'Connor DS, Garcia-Cardena G, McCabe TJ, Sessa WC. Reconstitution of an endothelial nitric-oxide synthase (eNOS), hsp90, and caveolin-1 complex in vitro. Evidence that hsp90 facilitates calmodulin stimulated displacement of eNOS from caveolin-1. The Journal of biological chemistry. 2000;275(29):22268-72. Epub 2000/04/27.

36. Fleming I, Busse R. Molecular mechanisms involved in the regulation of the endothelial nitric oxide synthase. American journal of physiology Regulatory, integrative and comparative physiology. 2003;284(1):R1-12. Epub 2002/12/17.

37. McCabe TJ, Fulton D, Roman LJ, Sessa WC. Enhanced electron flux and reduced calmodulin dissociation may explain "calcium-independent" eNOS

activation by phosphorylation. The Journal of biological chemistry. 2000;275(9):6123-8. Epub 2000/02/29.

38. Daff S. NO synthase: structures and mechanisms. Nitric oxide : biology and chemistry / official journal of the Nitric Oxide Society. 2010;23(1):1-11. Epub 2010/03/23.

39. Crane BR, Arvai AS, Ghosh DK, Wu C, Getzoff ED, Stuehr DJ, et al. Structure of nitric oxide synthase oxygenase dimer with pterin and substrate. Science. 1998;279(5359):2121-6. Epub 1998/04/16.

40. Antoniades C, Shirodaria C, Leeson P, Antonopoulos A, Warrick N, Van-Assche T, et al. Association of plasma asymmetrical dimethylarginine (ADMA) with elevated vascular superoxide production and endothelial nitric oxide synthase uncoupling: implications for endothelial function in human atherosclerosis. European heart journal. 2009;30(9):1142-50. Epub 2009/03/20.

41. Vallance P, Leone A, Calver A, Collier J, Moncada S. Endogenous dimethylarginine as an inhibitor of nitric oxide synthesis. Journal of cardiovascular pharmacology. 1992;20 Suppl 12:S60-2. Epub 1992/01/01.

42. Roe ND, Ren J. Nitric oxide synthase uncoupling: a therapeutic target in cardiovascular diseases. Vascular pharmacology. 2012;57(5-6):168-72. Epub 2012/03/01.

43. Landmesser U, Dikalov S, Price SR, McCann L, Fukai T, Holland SM, et al. Oxidation of tetrahydrobiopterin leads to uncoupling of endothelial cell nitric oxide synthase in hypertension. The Journal of clinical investigation. 2003;111(8):1201-9.

44. Zhang L, Rao F, Zhang K, Khandrika S, Das M, Vaingankar SM, et al. Discovery of common human genetic variants of GTP cyclohydrolase 1 (GCH1)

governing nitric oxide, autonomic activity, and cardiovascular risk. The Journal of clinical investigation. 2007;117(9):2658-71. Epub 2007/08/25.

45. Lei J, Vodovotz Y, Tzeng E, Billiar TR. Nitric oxide, a protective molecule in the cardiovascular system. Nitric oxide : biology and chemistry / official journal of the Nitric Oxide Society. 2013;35:175-85. Epub 2013/10/08.

46. Rudic RD, Shesely EG, Maeda N, Smithies O, Segal SS, Sessa WC. Direct evidence for the importance of endothelium-derived nitric oxide in vascular remodeling. The Journal of clinical investigation. 1998;101(4):731-6. Epub 1998/03/21.

47. Casey DB, Pankey EA, Badejo AM, Bueno FR, Bhartiya M, Murthy SN, et al. Peroxynitrite has potent pulmonary vasodilator activity in the rat. Canadian journal of physiology and pharmacology. 2012;90(4):485-500. Epub 2012/03/29.

48. Ray R, Shah AM. NADPH oxidase and endothelial cell function. Clin Sci (Lond). 2005;109(3):217-26.

49. Li JM, Shah AM. Endothelial cell superoxide generation: regulation and relevance for cardiovascular pathophysiology. American journal of physiology Regulatory, integrative and comparative physiology. 2004;287(5):R1014-30. Epub 2004/10/12.

50. Breton-Romero R, Lamas S. Hydrogen peroxide signaling in vascular endothelial cells. Redox biology. 2014;2:529-34. Epub 2014/03/19.

51. Cai H. Hydrogen peroxide regulation of endothelial function: origins, mechanisms, and consequences. Cardiovascular research. 2005;68(1):26-36. Epub 2005/07/13.

52. Cohen G. Enzymatic/nonenzymatic sources of oxyradicals and regulation of antioxidant defenses. Annals of the New York Academy of Sciences. 1994;738:8-14. Epub 1994/11/17.

53. Bonomini F, Tengattini S, Fabiano A, Bianchi R, Rezzani R. Atherosclerosis and oxidative stress. Histology and histopathology. 2008;23(3):381-90. Epub 2007/12/12.

54. Babior BM, Lambeth JD, Nauseef W. The neutrophil NADPH oxidase. Archives of biochemistry and biophysics. 2002;397(2):342-4. Epub 2002/02/14.

55. Lassegue B, San Martin A, Griendling KK. Biochemistry, physiology, and pathophysiology of NADPH oxidases in the cardiovascular system. Circulation research. 2012;110(10):1364-90.

56. De Leo FR, Ulman KV, Davis AR, Jutila KL, Quinn MT. Assembly of the human neutrophil NADPH oxidase involves binding of p67phox and flavocytochrome b to a common functional domain in p47phox. The Journal of biological chemistry. 1996;271(29):17013-20. Epub 1996/07/19.

57. Schroder K. Isoform specific functions of Nox protein-derived reactive oxygen species in the vasculature. Current opinion in pharmacology. 2010;10(2):122-6. Epub 2010/02/13.

58. Bayraktutan U, Blayney L, Shah AM. Molecular characterization and localization of the NAD(P)H oxidase components gp91-phox and p22-phox in endothelial cells. Arteriosclerosis, thrombosis, and vascular biology. 2000;20(8):1903-11. Epub 2000/08/11.

59. Bedard K, Krause KH. The NOX family of ROS-generating NADPH oxidases: physiology and pathophysiology. Physiological reviews. 2007;87(1):245-313. Epub 2007/01/24.

60. Lapouge K, Smith SJ, Groemping Y, Rittinger K. Architecture of the p40-p47-p67phox complex in the resting state of the NADPH oxidase. A central role for p67phox. The Journal of biological chemistry. 2002;277(12):10121-8. Epub 2002/01/18.

61. Pendyala S, Usatyuk PV, Gorshkova IA, Garcia JG, Natarajan V. Regulation of NADPH oxidase in vascular endothelium: the role of phospholipases, protein kinases, and cytoskeletal proteins. Antioxidants & redox signaling. 2009;11(4):841-60. Epub 2008/10/03.

62. Fu XJ, Peng YB, Hu YP, Shi YZ, Yao M, Zhang X. NADPH oxidase 1 and its derived reactive oxygen species mediated tissue injury and repair. Oxidative medicine and cellular longevity. 2014;2014:282854. Epub 2014/03/29.

63. Lee CF, Qiao M, Schroder K, Zhao Q, Asmis R. Nox4 is a novel inducible source of reactive oxygen species in monocytes and macrophages and mediates oxidized low density lipoprotein-induced macrophage death. Circulation research. 2010;106(9):1489-97. Epub 2010/04/03.

64. Brandes RP, Schroder K. Composition and functions of vascular nicotinamide adenine dinucleotide phosphate oxidases. Trends in cardiovascular medicine. 2008;18(1):15-9. Epub 2008/01/22.

65. Bedard K, Jaquet V, Krause KH. NOX5: from basic biology to signaling and disease. Free radical biology & medicine. 2012;52(4):725-34. Epub 2011/12/21.

66. Singh U, Jialal I. Oxidative stress and atherosclerosis. Pathophysiology : the official journal of the International Society for Pathophysiology / ISP. 2006;13(3):129-42. Epub 2006/06/08.

67. Nunes SF, Figueiredo IV, Pereira JS, de Lemos ET, Reis F, Teixeira F, et al. Monoamine oxidase and semicarbazide-sensitive amine oxidase kinetic analysis in mesenteric arteries of patients with type 2 diabetes. Physiological

research / Academia Scientiarum Bohemoslovaca. 2011;60(2):309-15. Epub 2010/12/01.

68. Rouzer CA, Marnett LJ. Cyclooxygenases: structural and functional insights. Journal of lipid research. 2009;50 Suppl:S29-34. Epub 2008/10/28.

69. Droge W. Free radicals in the physiological control of cell function. Physiological reviews. 2002;82(1):47-95. Epub 2002/01/05.

70. Hamilton CA, Miller WH, Al-Benna S, Brosnan MJ, Drummond RD, McBride MW, et al. Strategies to reduce oxidative stress in cardiovascular disease. Clin Sci (Lond). 2004;106(3):219-34. Epub 2004/01/22.

71. Wassmann S, Wassmann K, Nickenig G. Modulation of oxidant and antioxidant enzyme expression and function in vascular cells. Hypertension. 2004;44(4):381-6. Epub 2004/09/01.

72. Vanhoutte PM, Shimokawa H, Tang EH, Feletou M. Endothelial dysfunction and vascular disease. Acta Physiol (Oxf). 2009;196(2):193-222. Epub 2009/02/18.

73. El-Gamal D, Rao SP, Holzer M, Hallstrom S, Haybaeck J, Gauster M, et al. The urea decomposition product cyanate promotes endothelial dysfunction. Kidney international. 2014. Epub 2014/06/19.

74. Komori K, Shimokawa H, Vanhoutte PM. Hypercholesterolemia impairs endothelium-dependent relaxations to aggregating platelets in porcine iliac arteries. Journal of vascular surgery. 1989;10(3):318-25. Epub 1989/09/01.

75. Vanhoutte PM, Feletou M, Taddei S. Endothelium-dependent contractions in hypertension. British journal of pharmacology. 2005;144(4):449-58. Epub 2005/01/19.

76. Shimokawa H, Vanhoutte PM. Impaired endothelium-dependent relaxation to aggregating platelets and related vasoactive substances in porcine coronary arteries in hypercholesterolemia and atherosclerosis. Circulation research. 1989;64(5):900-14. Epub 1989/05/01.

77. Eto Y, Shimokawa H, Fukumoto Y, Matsumoto Y, Morishige K, Kunihiro I, et al. Combination therapy with cerivastatin and nifedipine improves endothelial dysfunction after balloon injury in porcine coronary arteries. Journal of cardiovascular pharmacology. 2005;46(1):1-6. Epub 2005/06/21.

78. Borg-Capra C, Fournet-Bourguignon MP, Janiak P, Villeneuve N, Bidouard JP, Vilaine JP, et al. Morphological heterogeneity with normal expression but altered function of G proteins in porcine cultured regenerated coronary endothelial cells. British journal of pharmacology. 1997;122(6):999-1008. Epub 1997/12/24.

79. Kennedy S, Fournet-Bourguignon MP, Breugnot C, Castedo-Delrieu M, Lesage L, Reure H, et al. Cells derived from regenerated endothelium of the porcine coronary artery contain more oxidized forms of apolipoprotein-B-100 without a modification in the uptake of oxidized LDL. Journal of vascular research. 2003;40(4):389-98. Epub 2003/08/09.

80. Choi S, Park S, Liang GH, Kim JA, Suh SH. Superoxide generated by lysophosphatidylcholine induces endothelial nitric oxide synthase downregulation in human endothelial cells. Cell Physiol Biochem. 2010;25(2-3):233-40.

81. Zembowicz A, Tang JL, Wu KK. Transcriptional induction of endothelial nitric oxide synthase type III by lysophosphatidylcholine. The Journal of biological chemistry. 1995;270(28):17006-10.

82. Konopatskaya O, Whatmore JL, Tooke JE, Shore AC. Insulin and lysophosphatidylcholine synergistically stimulate NO-dependent cGMP production in human endothelial cells. Diabet Med. 2003;20(10):838-45.

83. Millanvoye-Van Brussel E, Topal G, Brunet A, Do Pham T, Deckert V, Rendu F, et al. Lysophosphatidylcholine and 7-oxocholesterol modulate Ca2+ signals and inhibit the phosphorylation of endothelial NO synthase and cytosolic phospholipase A2. The Biochemical journal. 2004;380(Pt 2):533-9. Epub 2004/03/03.

84. Riederer M, Ojala PJ, Hrzenjak A, Graier WF, Malli R, Tritscher M, et al. Acyl chain-dependent effect of lysophosphatidylcholine on endothelial prostacyclin production. Journal of lipid research. 2010;51(10):2957-66.

85. Schmidt K, Werner-Felmayer G, Mayer B, Werner ER. Preferential inhibition of inducible nitric oxide synthase in intact cells by the 4-amino analogue of tetrahydrobiopterin. Eur J Biochem. 1999;259(1-2):25-31.

86. Nazarewicz RR, Bikineyeva A, Dikalov SI. Rapid and specific measurements of superoxide using fluorescence spectroscopy. Journal of biomolecular screening. 2013;18(4):498-503. Epub 2012/11/30.

87. Waldeck-Weiermair M, Alam MR, Khan MJ, Deak AT, Vishnu N, Karsten F, et al. Spatiotemporal correlations between cytosolic and mitochondrial Ca(2+) signals using a novel red-shifted mitochondrial targeted cameleon. PloS one. 2012;7(9):e45917.

88. Laurindo FR, Fernandes DC, Santos CX. Assessment of superoxide production and NADPH oxidase activity by HPLC analysis of dihydroethidium oxidation products. Methods in enzymology. 2008;441:237-60.

89. Li H, Meininger CJ, Wu G. Rapid determination of nitrite by reversed-phase high-performance liquid chromatography with fluorescence detection. J Chromatogr B Biomed Sci Appl. 2000;746(2):199-207. Epub 2000/11/15.

90. Schroder K, Zhang M, Benkhoff S, Mieth A, Pliquett R, Kosowski J, et al. Nox4 is a protective reactive oxygen species generating vascular NADPH oxidase. Circulation research. 2012;110(9):1217-25.

91. Ojala PJ, Hermansson M, Tolvanen M, Polvinen K, Hirvonen T, Impola U, et al. Identification of alpha-1 acid glycoprotein as a lysophospholipid binding protein: a complementary role to albumin in the scavenging of lysophosphatidylcholine. Biochemistry. 2006;45(47):14021-31.

92. Tardivel S, Gousset-Dupont A, Robert V, Pourci ML, Grynberg A, Lacour B. Protective effects of EPA and deleterious effects of DHA on eNOS activity in Ea hy 926 cultured with lysophosphatidylcholine. Lipids. 2009;44(3):225-35.

93. Jia SJ, Jiang DJ, Hu CP, Zhang XH, Deng HW, Li YJ. Lysophosphatidylcholine-induced elevation of asymmetric dimethylarginine level by the NADPH oxidase pathway in endothelial cells. Vascular pharmacology. 2006;44(3):143-8.

94. Gharavi N, El-Kadi AO. Measurement of nitric oxide in murine Hepatoma Hepa1c1c7 cells by reversed phase HPLC with fluorescence detection. Journal of pharmacy & pharmaceutical sciences : a publication of the Canadian Society for Pharmaceutical Sciences, Societe canadienne des sciences pharmaceutiques. 2003;6(2):302-7. Epub 2003/08/26.

95. Heinloth A, Heermeier K, Raff U, Wanner C, Galle J. Stimulation of NADPH oxidase by oxidized low-density lipoprotein induces proliferation of human vascular endothelial cells. Journal of the American Society of Nephrology : JASN. 2000;11(10):1819-25. Epub 2000/09/27.

96. Watanabe N, Zmijewski JW, Takabe W, Umezu-Goto M, Le Goffe C, Sekine A, et al. Activation of mitogen-activated protein kinases by lysophosphatidylcholine-induced mitochondrial reactive oxygen species generation in endothelial cells. The American journal of pathology. 2006;168(5):1737-48.

97. Testa MP, Alvarado O, Wournell A, Lee J, Guilford FT, Henriksen SH, et al. Screening assay for oxidative stress in a feline astrocyte cell line, G355-5. Journal of visualized experiments : JoVE. 2011(53):e2841. Epub 2011/07/22.

98. Wolfram Kuhlmann CR, Wiebke Ludders D, Schaefer CA, Kerstin Most A, Backenkohler U, Neumann T, et al. Lysophosphatidylcholine-induced modulation of Ca(2+)-activated K(+)channels contributes to ROS-dependent proliferation of cultured human endothelial cells. Journal of molecular and cellular cardiology. 2004;36(5):675-82. Epub 2004/05/12.

99. Park CH, Kim MR, Han JM, Jeong TS, Sok DE. Lysophosphatidylcholine exhibits selective cytotoxicity, accompanied by ROS formation, in RAW 264.7 macrophages. Lipids. 2009;44(5):425-35.

100. Lin P, Welch EJ, Gao XP, Malik AB, Ye RD. Lysophosphatidylcholine modulates neutrophil oxidant production through elevation of cyclic AMP. J Immunol. 2005;174(5):2981-9.

101. Petry A, Djordjevic T, Weitnauer M, Kietzmann T, Hess J, Gorlach A. NOX2 and NOX4 mediate proliferative response in endothelial cells. Antioxidants & redox signaling. 2006;8(9-10):1473-84.

102. Heumuller S, Wind S, Barbosa-Sicard E, Schmidt HH, Busse R, Schroder K, et al. Apocynin is not an inhibitor of vascular NADPH oxidases but an antioxidant. Hypertension. 2008;51(2):211-7.

103. Virdis A, Bacca A, Colucci R, Duranti E, Fornai M, Materazzi G, et al. Endothelial dysfunction in small arteries of essential hypertensive patients: role of cyclooxygenase-2 in oxidative stress generation. Hypertension. 2013;62(2):337-44.

104. Facino RM, Carini M, Aldini G. Antioxidant activity of nimesulide and its main metabolites. Drugs. 1993;46 Suppl 1:15-21. Epub 1993/01/01.

105. Kim YL, Im YJ, Ha NC, Im DS. Albumin inhibits cytotoxic activity of lysophosphatidylcholine by direct binding. Prostaglandins Other Lipid Mediat. 2007;83(1-2):130-8.

106. Van Buul JD, Fernandez-Borja M, Anthony EC, Hordijk PL. Expression and localization of NOX2 and NOX4 in primary human endothelial cells. Antioxidants & redox signaling. 2005;7(3-4):308-17. Epub 2005/02/12.

107. Kuroda J, Nakagawa K, Yamasaki T, Nakamura K, Takeya R, Kuribayashi F, et al. The superoxide-producing NAD(P)H oxidase Nox4 in the nucleus of human vascular endothelial cells. Genes to cells : devoted to molecular & cellular mechanisms. 2005;10(12):1139-51. Epub 2005/12/06.

108. Ago T, Kuroda J, Pain J, Fu C, Li H, Sadoshima J. Upregulation of Nox4 by hypertrophic stimuli promotes apoptosis and mitochondrial dysfunction in cardiac myocytes. Circulation research. 2010;106(7):1253-64. Epub 2010/02/27.

109. Croset M, Brossard N, Polette A, Lagarde M. Characterization of plasma unsaturated lysophosphatidylcholines in human and rat. Biochemical Journal. 2000;345 Pt 1:61-7.

110. Sprong H, van der Sluijs P, van Meer G. How proteins move lipids and lipids move proteins. Nature reviews Molecular cell biology. 2001;2(7):504-13. Epub 2001/07/04.

111. Fleming I. Molecular mechanisms underlying the activation of eNOS. Pflugers Archiv : European journal of physiology. 2010;459(6):793-806. Epub 2009/12/17.

112. Meyer zu Heringdorf D, Jakobs KH. Lysophospholipid receptors: signalling, pharmacology and regulation by lysophospholipid metabolism. Biochimica et biophysica acta. 2007;1768(4):923-40. Epub 2006/11/03.

113. Xu Y. Sphingosylphosphorylcholine and lysophosphatidylcholine: G protein-coupled receptors and receptor-mediated signal transduction. Biochimica et biophysica acta. 2002;1582(1-3):81-8. Epub 2002/06/19.

APPENDIX

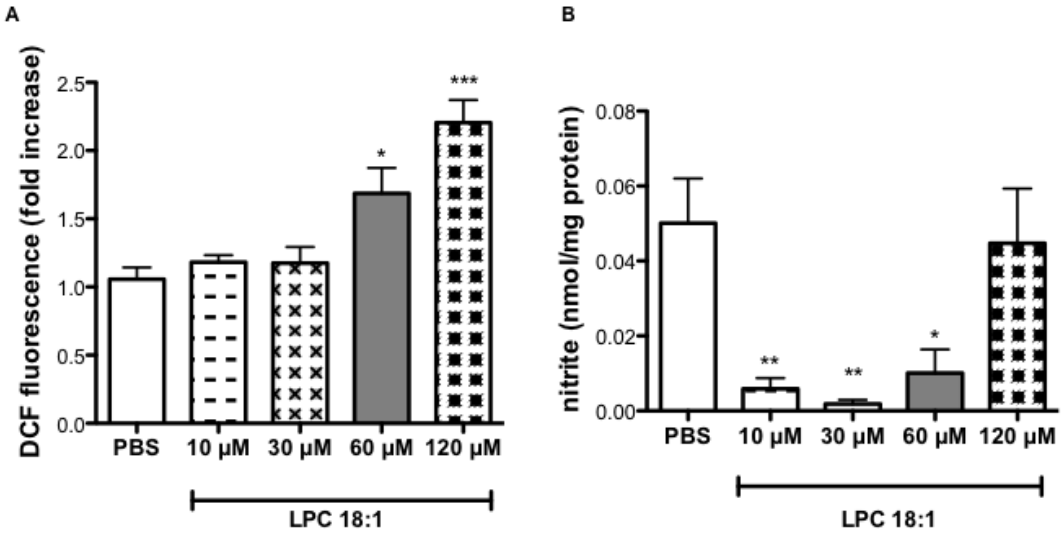

Supplementary figure 1. Dose response effect of LPC 18:1 on intracellular ROS formation and nitrite levels. A) EA.hy926 cells were preincubated with 10µM H_2DCFDA fluorescent dye, after which they were treated with various concentration of LPC 18:1 or vehicle control (PBS) in 5% FBS medium for 15 minutes. Thereafter, cells were lysed and fluorescence was measured. B) Cells were treated with various concentration of µM LPC 18:1 and vehicle control (PBS) with or without 100 µM eNOS inhibitor L-NNA in 5% FBS-containing medium for 15 minutes, after which medium was collected, and protein lysates were used for normalization. Nitrite was measured with HPLC. Results shown are mean ± SEM, of 3 independent experiments performed in triplicates and analyzed by one-way ANOVA with Tukey's post-hoc test. If otherwise not indicated, asterisks show significance compared to PBS control (*p<0,05, **p<0,01, ***p<0,001).

PUBLICATIONS

Kozina A, Opresnik S, Sze Ka Wong M, Hallström S, Graier WF, Malli R, Schröder K, Schmidt K, Frank S. Oleoyl-lysophosphatidylcholine limits endothelial nitric oxide bioavailability by induction of reactive oxygen species. PLOS ONE. 2014 Manuscript accepted for publication 6th of November 2014.

El-Gamal D, Rao SP, Holzer M, Hallström S, Haybaeck J, Gauster M, Wadsack C, Kozina A, Frank S, Schicho R, Schuligoi R, Heinemann A, Marsche G. The urea decomposition product cyanate promotes endothelial dysfunction. Kidney International. 2014. Epub 18 June 2014; doi:10.1038/ki.2012.218

CURRICULUM VITAE

Andrijana Kozina, MSc

Personal

Date of birth 28 July 1986, Zadar, Croatia

Affiliation Institute of Molecular Biology and Biochemistry
Medical University of Graz
Harrachgasse 21/III
A-8010 Graz, Austria
Tel: +43 (316) 380 4483
andrijana.kozina@medunigraz.at

Education

2011-2014	PhD program Molecular Medicine Institute of Molecular Biology and Biochemistry Medical University of Graz, Austria
2010	MSc in Molecular Biology Faculty of Science, University of Zagreb, Croatia
2008	BSc in Molecular Biology Faculty of Science, University of Zagreb, Croatia

Presentations

Kozina, A; Opresnik, S; Hallström, S; Schmidt, K; Malli, R; Graier, WF; Frank, S. Acyl-chain dependent effect of lysophosphatidylcholine on endothelial nitric oxide synthase and NO bioavailability in endothelial cells. 82nd EAS Congress Madrid, Spain. May 31st-June 3rd 2014. [Poster]

Kozina, A; Opresnik, S; Hallström, S; Schmidt, K; Malli, R; Graier, WF; Frank, S. Acyl-chain dependent effect of lysophosphatidylcholine on endothelial nitric oxide synthase and NO bioavailability in endothelial cells. 21st Annual Meeting of the Austrian Atherosclerosis Society. St. Gilgen/ Wolfgangsee, Austria. May 9-10th, 2014. [Oral communication]

Kozina, A; Opresnik, S; Rao, SP; Hrzenjak, A; Hallström, S; Sreckovic, I; Holzer, M; Marsche, G; Birner-Gruenberger, R; Stojakovic, T; Scharnagl, H; Frank, S. Endothelial lipase attenuates vasorelaxing capacity of HDL. 21st Annual Meeting of the Austrian Atherosclerosis Society. St. Gilgen/ Wolfgangsee, Austria. May 9-10th, 2014. [Oral communication]

Kozina, A; Opresnik, S; Hallström, S; Frank, S. Acyl-chain dependent effect of lysophosphatidylcholine on endothelial nitric oxide synthase (eNOS) and NO bioavailability in endothelial cells. “Doctoral Day” Medical University of Graz. Graz, Austria, December 9th 2013. [Poster]

Kozina, A; Patankar, JV; Frank, S. Transcriptional regulation of intestinal fatty acid translocase/CD36 expression by GATA4. “Doctoral Day” Medical University of Graz. Graz, Austria, December 7th, 2012. [Poster]

Conferences

82nd EAS Congress Madrid, Spain. May 31st-June 3rd 2014. [Poster]

21st Annual Meeting of the Austrian Atherosclerosis Society. St. Gilgen/ Wolfgangsee, Austria. May 9-10th, 2014. [Oral communication]

“Doctoral Day” Medical University of Graz. Graz, Austria, December 9th 2013. [Poster]

20th Annual Meeting of the Austrian Atherosclerosis Society. St. Gilgen/ Wolfgangsee, Austria. May 10-11th, 2013.

“Doctoral Day” Medical University of Graz. Graz, Austria, December 7th, 2012. [Poster]

“Doctoral Day” Medical University of Graz “PhD Program Molecular Medicine”. Graz, Austria. November 4th, 2011.